Walther-Straub-Institut für Pharmakologie und Toxikologie

der Ludwig-Maximilians-Universität München

Vorstand: Prof. Dr. Thomas Gudermann

Mode of action of the mitochondrial Ca^{2+} uptake enhancer efsevin for treatment of cardiac arrhythmia

Dissertation

zum Erwerb des Doktorgrades der Naturwissenschaften

an der Medizinischen Fakultät der

Ludwig-Maximilians-Universität zu München

Vorgelegt von

Fabiola Charlotte Wilting

aus

Titisee-Neustadt

2022

Mit Genehmigung der Medizinischen Fakultät

der Universität München

Betreuer(in):	Prof. Dr. Annette Nicke
Zweitgutachter:	Prof. Dr. Martin Biel
Dekan:	Prof. Dr. Thomas Gudermann
Tag der mündlichen Prüfung:	03.02.2023

1 Affirmation

LMU LUDWIG-MAXIMILIANS-UNIVERSITÄT MÜNCHEN | Promotionsbüro Medizinische Fakultät | MMRS

Eidesstattliche Versicherung

Wilting, Fabiola Charlotte

_____

Name, Vorname

Ich erkläre hiermit an Eides statt, dass ich die vorliegende Dissertation mit dem Titel:

Mode of action of the mitochondrial Ca^{2+} uptake enhancer efsevin for treatment of cardiac arrhythmia

selbständig verfasst, mich außer der angegebenen keiner weiteren Hilfsmittel bedient und alle Erkenntnisse, die aus dem Schrifttum ganz oder annähernd übernommen sind, als solche kenntlich gemacht und nach ihrer Herkunft unter Bezeichnung der Fundstelle einzeln nachgewiesen habe.

Ich erkläre des Weiteren, dass die hier vorgelegte Dissertation nicht in gleicher oder in ähnlicher Form bei einer anderen Stelle zur Erlangung eines akademischen Grades eingereicht wurde.

München, 05.07.2023 — Fabiola Wilting

Ort, Datum — Unterschrift
Doktorandin bzw. Doktorand

2 Abbreviations

$[Ca^{2+}]_I$	intracellular free Ca^{2+} concentration
$[Ca^{2+}]_m$	intra-mitochondrial Ca^{2+} concentration
°C	centigrade
AP	action potential
ADP/ATP	adenosine diphosphate/ adenosine triphosphate
BLM	Black lipid membrane
Ca^{2+}	calcium
$CaCl_2$	calcium chloride
CICR	calcium-induced calcium release
CPVT	catecholaminergic polymorphic ventricular tachycardia
CVD	cardiovascular disease
EC	excitation-contraction
h	hour
IMM	inner mitochondrial membrane
KO	knock out
LTCC	L-type calcium channel
MCUC	mitochondrial calcium uniporter complex
min	minute
ml	milliliter
mM	millimolar
mVDAC2	murine voltage dependent anion channel
NCX	Na^+/ Ca^{2+} exchanger
OMM	outer mitochondrial membrane

RyR	ryanodine receptor
SERCA	sarcoplasmatic/endoplasmatic reticulum calcium-ATPase
SR	sarcoplasmatic reticulum
tre	*tremblor*
V	volt
VDAC	voltage dependent anion channel
vs	versus
zVDAC	zebrafish voltage dependent anion channel
µM	micromolar

3 Publication list

This cumulative thesis is based on the following peer-reviewed publications by the author:

- Wilting F, Kopp R, Gurnev PA, Schedel A, Dupper NJ, Kwon O, Nicke A, Gudermann T, Schredelseker J. The antiarrhythmic compound efsevin directly modulates voltage-dependent anion channel 2 by binding to its inner wall and enhancing mitochondrial Ca^{2+} uptake. *Br J Pharmacol*. February 2020:bph.15022. doi:10.1111/bph.15022
- Schweitzer MK, Wilting F, Sedej S, Dreizehner L, Dupper NJ, Tian Q, Moretti A, My I, Kwon O, Priori SG, Laugwitz KL, Storch U, Lipp P, Breit A, Mederos y Schnitzler M, Gudermann T, Schredelseker J. Suppression of Arrhythmia by Enhancing Mitochondrial Ca^{2+} Uptake in Catecholaminergic Ventricular Tachycardia Models. JACC Basic to Transl Sci. 2017;2(6). doi:10.1016/j.jacbts.

4 Introduction

Cardiovascular diseases (CVDs) produce immense health and economic burdens in Europe and globally and will continue to dominate mortality[1,2]. According to the World Health Organisation (WHO)[3], it has been estimated that CVDs are responsible for 17.9 million deaths each year. This represents 31% of all global deaths. In Europe, CVDs cause around 4 million deaths annually, accounting for 45% of all deaths[4]. By comparison, cancer, the next most common cause of death, accounts for just under 2 million deaths (22%)[2]. Among heart diseases, severe cardiac arrhythmias are with approximately one-half of all cardiovascular deaths the most harmful[5].

Despite these alarming facts, pharmacological treatment options for arrhythmia are still very limited. The most currently used antiarrhythmic drugs are classified based on their target and can be divided into four classes[6]: (i) sodium-channel blockers, (ii) beta-blockers, (iii) potassium channel blockers, and (iv) Ca^{2+} channel blockers. By directly or indirectly influencing ion channels in the sarcolemma, they block the expansion of arrhythmic events along the heart muscle (myocardium). But due to their ability to modulate the cardiac action potential (AP), the existing drugs often have proarrhythmic or negative inotropic side effects, coupled with a very narrow therapeutic range[6,7]. The most dangerous side effect is their ability to produce new arrhythmias. Possible mechanism for these arrhythmias can be an abnormal impulse formation, like the production of early after depolarizations (EADs) in case of class III agents or conduction disturbances in case of class I and III agents, which lead to reentry circuits. This occurs through a deceleration of cardiac conduction, with the result that APs reactivate tissue that has recovered from refractoriness[7]. Thus, with the exception of ß-blockers, none of the commonly used antiarrhythmics can be deployed for long-term treatment. These facts limit their use in the medication of CVDs. As a consequence, there is an urgent need for the development of new therapeutic approaches.

To overcome the aforementioned problems, intracellular structures are in the center of current research. A special focus lies on the intracellular Ca^{2+} signaling network, since cardiac contractility and rhythmicity critically depend on intracellular Ca^{2+} levels[8]. Additionally, many CVDs, including heart failure and many arrhythmias, are related to defects in cardiac Ca^{2+} handling and cellular Ca^{2+} homeostasis[9]. To ensure proper cardiac contractility and rhythmicity Ca^{2+} handling in cardiomyocytes is tightly regulated by a sub-cellular network of multiple proteins, pathways and organelles (**Fig. 1**). The

excitation of a cardiac muscle cell by an AP results in electrophysiological depolarization of the cell membrane. Contraction, on the other hand, is a biomechanical process that takes place at the contractile structures inside the cell. The mechanisms that cause the coupling between membrane depolarization and contraction are summarized under the term excitation-contraction (EC) coupling. When cardiomyocytes are depolarized Ca^{2+} enters through the L-type calcium channel (LTCC) in the sarcolemma of the T-tubuli. This entry of Ca^{2+} triggers via intracellular calcium channels called ryanodine receptors (RyR), the release of further calcium stored in the sarcoplasmic reticulum (SR). RyR2 represents the cardiomyocyte-specific isoform and the channels are located in close vicinity (20nm) to the LTCCs[8]. The calcium explosion is called calcium-induced calcium release (CICR), representing an efficient amplification mechanism, and triggering the contraction.

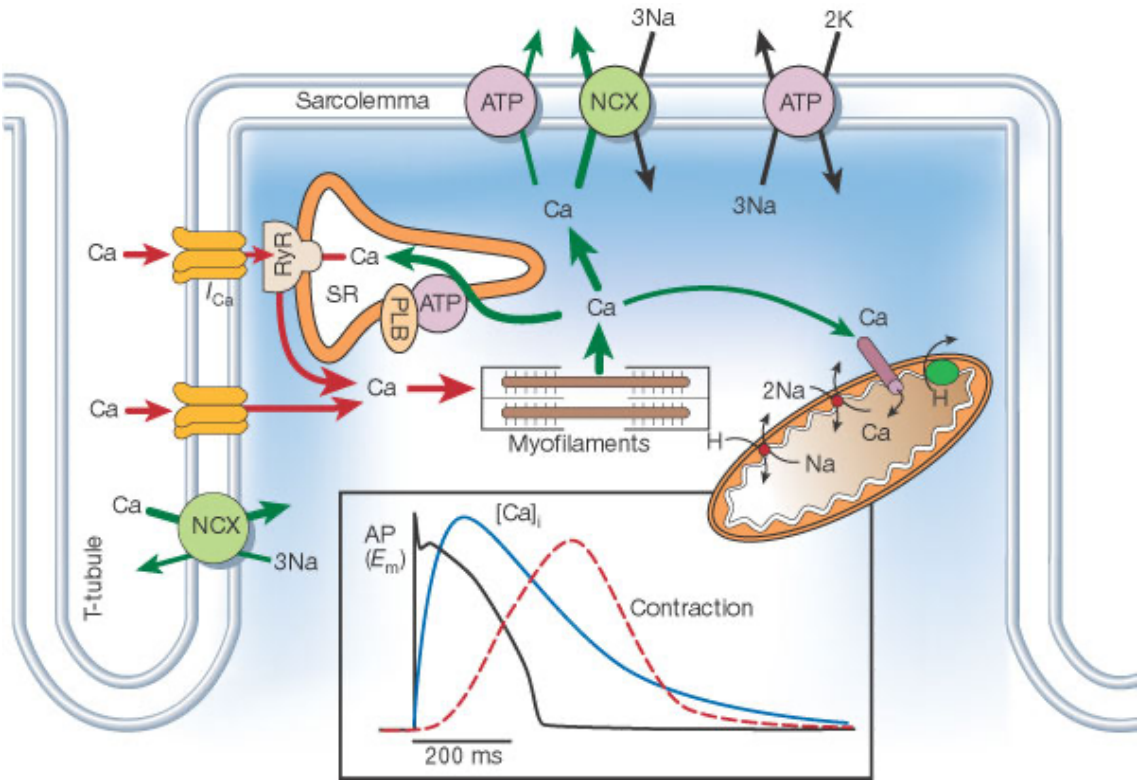

Figure 1: Schematic of Ca^{2+} signaling proteins and events in adult cardiomyocytes[8]

During the systole Ca^{2+} enters through the L-type calcium channel (I_{Ca}), and activates the ryanodine receptor (RyR) to release the Ca^{2+} contents of the SR (red arrows). Ca^{2+} released from the internal store together with Ca^{2+} entering from I_{Ca} causes a rise in intracellular free Ca^{2+} that binds to troponin C (myofilaments) to cause contraction. During the diastole Ca^{2+} is then extruded from the cell via the Na^{+}/Ca^{2+} exchanger (NCX), shuffled back into the SR via calcium-ATPase (SERCA) and transported to a yet unknown extend into mitochondria via the mitochondrial Ca^{2+} uniporter. This restores basal Ca^{2+} levels (green arrows). Opening of RyRs during the diastole can induce similar mechanisms and lead to arrythmia.

Insert: Time response curves showing action potential (AP), Ca^{2+} current ($[Ca]_i$]) and contraction (Copyright: with permission: license number 4580670753852).

The release from the internal store, in conjunction with Ca^{2+} entering through LTCC, cause a rise in intracellular free Ca^{2+} ($[Ca^{2+}]_i$) allowing Ca^{2+} to bind to troponin C, which leads to contraction of the cardiomyocyte[8]. At the peak of the Ca^{2+} response (~100 ms after stimulation) the cytosolic Ca^{2+} signal can reach ~1 µM. However, due to the heterogeneous propagation within the cytosol, the Ca^{2+} concentration decreases with increasing distance from the SR[10,11]. For relaxation $[Ca^{2+}]_i$ has to decline back to resting conditions to allow Ca^{2+} to dissociate from troponin. A small part of Ca^{2+} is transferred out of the cell via the Na^+/ Ca^{2+} exchanger (NCX). The major fraction recirculates back into the SR via the sarco/endoplasmatic reticulum calcium-ATPase (SERCA) as the cardiomyocyte relaxes and the Ca^{2+} concentration of the cytosol returns to a normal prestimulated level of ~100nM[11]. These recurring peaks and declines in $[Ca^{2+}]_i$ are published as Ca^{2+} transients[8,12,13]. During the diastole it is crucial that the Ca^{2+} homeostasis is maintained. In many CVDs, the storage of calcium is disturbed. Spontaneous diastolic release of Ca^{2+} from the SR can lead to sparks, causing positive feedback calcium waves which triggers CVDs like arrhythmias.

Apart from the aforementioned big players like SERCA and NCX, many other Ca^{2+} transporters exist in cardiomyocytes to fine tune this process. Interestingly, during relaxation a small fraction of systolic Ca^{2+} (ca.1-2%)[14] is also taken up by mitochondria, which thereby shape the kinetics of the Ca^{2+} transients. However, this mechanism has not been studied intensively, although recent studies suggest that it has modulatory and regulatory capabilities.

Mitochondria are primarily vital for the energy supply of the cell, but also play a substantial, yet barely acknowledged role in cellular Ca^{2+} handling. The heart possesses the highest content of mitochondria of any tissue comprising 36% of the total intracellular volume of a mammalian cardiomyocyte[15,16] (**Fig. 2**). In cardiomyocytes, mitochondria are in close contact with the SR and are thus in close proximity to the Ca^{2+} release sites of the SR[17]. Studies showed that this spatial proximity leads to Ca^{2+}-mediated interactions between the two structures[18]. The mitochondrial wall consists of two biomembranes that create two separate mitochondrial compartments: the mitochondrial intermembrane space (MIMS) and the mitochondrial matrix. The outer mitochondrial membrane (OMM) consists mainly of phospholipids: phosphatidylcholine, phosphatidylethanolamine,

phosphatidylinositol[19]. The inner mitochondrial membrane (IMM) forms a surface greatly enlarged by folds (cristae) or tubuli. Their general function is to provide adenosine triphosphate (ATP), which is achieved primarily through oxidative respiratory phosphorylation[20]. This metabolic activity has to be synchronized in time and intensity to the contractile activity of the cardiomyocytes. Under higher workload, the fast cytosolic Ca^{2+} transients are slowly integrated into the mitochondrial matrix by mitochondrial Ca^{2+} uptake. This results in a gradual increase of the mitochondrial Ca^{2+} concentration ($[Ca^{2+}]_m$), which activates proteins of the tricarboxylic acid cycle (TCA) cycle and thus energy production[21].

Moreover, recent studies showed fast beat-to-beat oscillations of mitochondrial Ca^{2+} though the physiological relevance of this is discussed controversially [22,23]. According to these studies, Ca^{2+} is rapidly transported into the mitochondrial matrix, which is reflected by fast transients of $[Ca^{2+}]_m$[21]. This mechanism, however, has not been investigated intensively although recent studies have indicated that it has greater modulatory capabilities than initially expected[24,25]. In the light of the important role of intracellular Ca^{2+} handling in cardiac physiology and pathophysiology, the mitochondrial Ca^{2+} network bears the potential to provide pharmacological target structures for the treatment of CVDs.

We and others have recently shown that an OMM channel, namely the voltage-dependent-anion-chanel 2 (VDAC2) transports Ca^{2+} into the MIMS and that this also happens in a fast way[26,27] The Ca^{2+} uptake into the matrix is then mainly driven by the mitochondrial calcium uniporter complex (MCUC)[28,29].

Recently our lab identified the synthetic compound efsevin, a dihydropyrrole carboxylic ester, in a chemical suppressor screen set up to identify new targets for cardiac arrhythmia and modulators for them. Specifically, efsevin recovered the rhythmic contractions of the heart in zebrafish embryos of the mutant line *tremblor*[30,31], which normally manifest uncoordinated irregular cardiac contractions due to a NCX null mutation[26]. In a pull-down assay, efsevin was demonstrated to specifically interact with VDAC2[26]. To test whether the antiarrhythmic effect is really attributable to the interaction of efsevin with VDAC2, cardiac rhythmicity was analyzed in VDAC2 *tremblor* embryos in which VDAC2 was either overexpressed or knocked down. Indeed, VDAC2 knock-down was shown to abolish the effect of efsevin, whereas VDAC2 overexpression showed the same rescuing

effect as efsevin treatment. These results establish VDAC2 as a hitherto unknown modulator of cardiac rhythmicity and a promising target for potential drugs for the treatment of cardiac arrhythmia. The close interaction of VDAC2 with the RyRs together with latest findings suggest that VDAC2 is a key player in mitochondrial Ca^{2+} handling.

VDACs are the most ubiquitous proteins in the OMM[32]. They are formed by a β-barrel with an α-helix lying inside a wide pore with an internal diameter of 1.5-4 nm[33–37]. Due to their large pore size, their role as selective ion transporters is questionable. However, experiments have shown the regulatory capacity of VDACs on Ca^{2+}, even if the exact mechanism remained unclear[29,38,39]. The name voltage-dependent anion channel originates from experiments in planar lipid bilayers where voltage-dependent gating of the channel was observed. However, it is still unclear if voltage represents the physiological trigger of channel gating *in vivo*. Higher eukaryotes express three distinct isoforms of VDAC: VDAC1-3, with a molecular weight of 32–34 kDa and approximately 75% sequence similarity. Data based on expression patterns and VDAC KO mice indicate a specific role of VDAC2 in cardiomyocytes[40,41]. The first 3D-structures of VDAC were obtained independently by three groups in 2008[36,37,42] by solving the structure of VDAC1. 7 years later, in 2015, the first crystal structure of a second VDAC isoform, namely zVDAC2[34] was resolved and showed high similarities with the published X-ray structures of murine and human VDAC1. zVDAC2 is a 19-stranded β-barrel with an N-terminal α-helix located within the pore of the channel **(Fig. 3)**. The barrel wall is formed by antiparallel β-strands, with parallel interactions of strand 1 and 19 that close the barrel. The maximum height and width of zVDAC2 is 35Å and 40Å respectively[34]. Due to their localization in the OMM, the VDACs are not easily accessible for electrophysiological studies. To investigate its channel properties, VDAC2 was reconstituted into a planar lipid bilayer membrane, called black lipid membranes (BLMs)[32]. When embedded in a bilayer, VDAC2 forms a high-conductance channel, which alters its selectivity and permeability by switching between different conformations induced by voltage. Thereby, VDAC2 shows a symmetrical conductance-voltage relationship. In 1M KCl and at low potentials of 0 to approximately +/-30 mV, the channel has its highest conductivity of 4-4.5 nS (classical “open” state) and is permeable to anions such as chloride, phosphates, adenine nucleotides and other anionic metabolites. At higher potentials (>+/-30-60 mV) the conductivity of VDAC2 is reduced by 50-60 % and the channel switches between several low conductance states (classical “closed” states). Under these conditions, the selectivity

of the channel changes so that the channel is less selective for anions and almost impermeable to ADP and ATP. This observed conductivity transition is reversible[35]. While there is broad agreement on the character of the classical open state, opinions on the closed state are very divergent[43–45]. Further research is therefore needed to fully clarify the behavior of VDAC2.

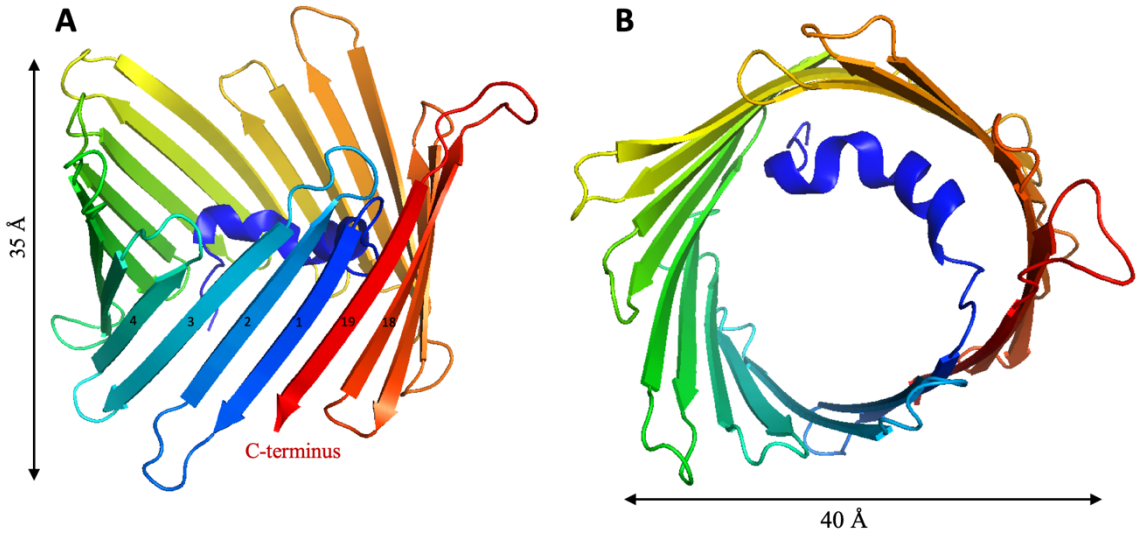

Figure 2: Overall structure of zVDAC2[34]

Schematic representations of zebrafish VDAC2 perpendicular to the membrane plane (**A**) and in the membrane plane (**B**) are shown. The protein scaffold is shown from the N-terminus (blue) to the C-terminus (red) in rainbow colours. **(**Copyright: created with PyMol)

4.1 Aim of this thesis

Previous data suggest that VDAC2 is regulated by efsevin, however the exact mode of action is still not understood. Therefore, this thesis seeks to investigate its molecular mode of action and its potential use for the treatment of cardiac arrhythmia. My hypothesis is that mitochondria represent an additional Ca^{2+} buffering compartment, thereby regulating Ca^{2+} homeostasis. By modulating VDAC2 conformational changes with efsevin and enhancing Ca^{2+} uptake, mitochondria can have a shaping effect on the intracellular calcium level and lead to a spacial and temporal restriction of diastolic Ca^{2+} sparks. Ca^{2+} from the SR, which is released by spontaneous sparks, is increasingly pumped into the mitochondria, which prevents an uncontrolled Ca^{2+} wave. And by preventing spontaneous and unintended waves, arrhythmias can be suppressed. Due to the low Ca^{2+} conductivity compared to SERCA, smaller events are prevented, but this mechanism has no effect on the regular Ca^{2+} cycle.

In my publications, I have handled the following questions. In a first step (i), I addressed the question, whether the Ca^{2+} conductance of VDAC is the relevant underlying mechanism for the observed effects by comparing results obtained with efsevin with those obtained with a known enhancer of mitochondrial Ca^{2+} uptake. In a second step (ii), I directly assessed the efsevin-induced changes in VDAC Ca^{2+} conductance by biochemical and biophysical approaches.

(i) Is the anti-arrhythmic effect limited to VDAC2-targeting drugs or can it also be achieved by activating IMM channels such as the MCUC?
   a. Paper 1: Suppression of Arrhythmia by Enhancing Mitochondrial Ca^{2+} Uptake in Catecholaminergic Ventricular Tachycardia Models

(ii) What is the molecular mechanism of the efsevin action? Although the capability of VDAC2 to suppress arrhythmic events could be proven experimentally, nothing is known about the molecular mechanisms of the efsevin – VDAC2 interactions. It is yet not clear whether efsevin directly interacts with VDAC2. Therefore, I tried to clarify if efsevin is able to modulate the electrophysiological properties of VDAC2 or if the measured effects require a yet unidentified protein partner.
   a. Paper 2: The antiarrhythmic compound efsevin directly modulates voltage-dependent anion channel 2 by binding to its inner wall and enhancing mitochondrial Ca^{2+} uptake

By answering these questions, I was able to establish efsevin as a new drug that specifically targets VDAC2 and confirms mt-Ca^{2+} uptake as a novel promising mechanism to treat cardiac arrhythmias.

Paper 1: Suppression of Arrhythmia by Enhancing Mitochondrial Ca^{2+} Uptake in Catecholaminergic Ventricular Tachycardia Models

Mitochondria have been identified as being responsible for regulating cardiac rhythm, but their potential as therapeutic targets have not been further explored. To establish fast mitochondrial Ca^{2+} uptake as the mode of action of efsevin, an enhancer of VDAC2 and kaempferol, an enhancer of the MCUC were used. I could proof, that both efsevin and kaempferol enhance fast calcium uptake by measuring the mitochondrial Ca^{2+} in a mouse cardiomyocyte cell line. To show that the increased Ca^{2+} uptake leads to an anti-arrhythmic effect, both substances were also tested in isolated $RyR2R^{4496C/WT}$ ventricular cardiomyocytes (*However, here I have performed only the kaempferol experiments)*. I could demonstrate that enhancing mitochondrial Ca^{2+} (mt-Ca^{2+}) uptake suppresses arrhythmia in $RyR2R^{4496C/WT}$ cardiomyocytes *in vitro* and proof that the effect is not limited to cell lines.

Within this publication I performed the following experiments:

- For this work, I have successfully established the cell-based calcium assay. In the cardiac muscle cell line HL-1, I could show that efsevin and kaempferol increased in a dose-dependent and significant manner the fast uptake of Ca^{2+}'into mitochondria. By using different Ca^{2+} chelators I could prove that Ca^{2+} is directly shuttled from the SR into mitochondria in a µm range.
- In a second step, I measured the antiarrhythmic effect of kaempferol by using isolated ventricular cardiomyocytes of mice that suffered from CPVT, due to a mutation in the gene for the RyR2. After application of isoprenaline, a catecholaminergic stimulus, the isolated cardiomyocytes showed a higher frequency of spontaneous diastolic Ca^{2+} release, so called Ca^{2+} waves. These waves could be suppressed by the addition of kaempferol. Thereby, I was able to establish mitochondria as a universal buffer system for the prevention of arrhythmias.

Paper 2: The antiarrhythmic compound efsevin directly modulates voltage dependent anion channel 2 by binding to its inner wall and enhancing mitochondrial Ca^{2+} uptake

It is assumed that VDAC2s, as large pore-forming proteins, allow free passage of ions, specifically Ca^{2+} and can selectively control only the passage of large molecules. To address this issue, recombinant zebrafish VDAC2 (zVDAC2) protein was purified and inserted it into BLMs. A direct effect of efsevin on both channel gating and opening probability was shown. Efsevin causes a shift of VDAC2 to the more anion-selective, closed state. These results indicate a direct efsevin-VDAC2 interaction, which has not yet been experimentally proven. However, this experiment could not provide any information about the molecular interactions. Therefore, protein-ligand docking was performed, in which the most likely binding site of efsevin on VDAC2 is calculated based on their molecular structures. A binding site was identified between the α-helix and the channel wall with the three amino acid residues N207, K236 and N238 as anchor points. Replacement of the three amino acid residues with alanines ($zVDAC2^{AAA}$) resulted in a complete loss of the efsevin effect on VDAC2.

However, since the efsevin insensitivity of the mutant was only shown in an isolated system, the question was whether these biophysical results could also be reproduced in a cellular system. For this purpose, wild-type zVDAC2 and the $zVDAC2^{AAA}$ mutant were heterologously expressed in cultured HL-1 cardiomyocytes. By measuring the altered mitochondrial Ca^{2+} uptake, it was confirmed that efsevin has also in a cellular system no effect on $zVDAC2^{AAA}$.

Taken together, the connection of efsevin with increased Ca^{2+} uptake clarified the antiarrhythmic effect electrophysiologically and provides new insights into the functioning of zVDAC2.

Within this publication I performed the following experiments:

- To investigate the molecular nature of the efsevin-VDAC2 interaction, I incorporated purified zVDAC2 protein into planar lipid bilayers and measured the electrophysical properties of zVDAC2 in the presence and absence of efsevin. For this work, I established both the purification of the channels and the bilayer measurements myself.
- Based on the molecular docking from Robin Kopp, I replaced the identified efsevin binding residues by alanine, and characterized the zVDAC2 mutant

biophysically. Thereby, I proved that alterations of the identified binding site effectively abolish efsevin's potential to control VDAC2 functions.

- To assess the physiological impact of efsevin-induced functional changes in VDAC2, I heterologously expressed wild-type zVDAC2 and the zVDAC2^{AAA} mutant in cultured HL-1 cardiomyocytes. By using my established calcium assay to measure the transfer of Ca^{2+} from the SR into the mitochondria, I could show that efsevin increases the fast Ca^{2+} uptake only in wild-type zVDAC2-transfected HL-1 cardiomyocytes.

5 Summary

Cardiovascular diseases (CVDs) like arrhythmia cause immense health and economic burdens in Europe and worldwide and are the number one cause of death worldwide. Mitochondria have been shown to act as regulators of cardiac rhythm, but their potential as therapeutic targets in the treatment of CVDs has not been further investigated. Recently, the synthetic compound efsevin was identified as a potent candidate drug for the treatment of cardiac arrhythmia due to its suppressive effect on arrhythmia in a zebrafish model. Its antiarrhythmic activity was linked to an interaction with the voltage-dependent anion channel 2 (VDAC2), a pore-forming channel in the outer mitochondrial membrane (OMM). VDAC2 facilitates the transport of a variety of metabolites and ions, including Ca^{2+}, through the OMM. However, its potential to directly modulate calcium transport into the mitochondria was questionable due to its large pore size.

In this work, the mode-of-action of efsevin was characterized. I could proof in a cardiomyocyte cell line, that efsevin leads to increased fast Ca^{2+} uptake into the mitochondria. This increased Ca^{2+} calcium uptake was linked to an anti-arrhythmic effect and confirmed in freshly isolated $RyR^{2R4496C/WT}$ cardiomyocytes.

In addition, the efsevin-VDAC2 interaction was biophysically described. It was shown that efsevin modulates the open probability of VDAC2 and stabilizes the channel in its cation-selective closed state. Molecular ligand-protein docking was used to identify the binding site of efsevin on the inner wall of the channel, adjacent to the N-terminal α-helix. The binding site is formed by amino acids N207, K237, and N238. Replacement of these three amino acids with alanines abolished the efsevin sensitivity of the channel. This biophysical effect was also demonstrated in cultured murine cardiomyocytes in which either wild-type zVDAC2 or the efsevin-insensitive zVDAC2AAA mutant were overexpressed. Both channels, wild-type zVDAC2 and the zVDAC2AAA mutant, restored mitochondrial Ca^{2+} uptake. However, only wild-type zVDAC2 was sensitive to efsevin leading to an increased mitochondrial Ca^{2+} uptake.

In conclusion, in this work, I established pharmacological modulation of fast mitochondrial Ca^{2+} uptake as a possible pharmacological target and was able to show the capability of zVDAC2 to modulate Ca^{2+} levels. Deciphering the direct interaction of efsevin and zVDAC2 reveals new insights into cardiomyocyte functioning and provides

the basis for the computer-aided development of optimized molecules that could function as tools in research and ultimately as therapeutics for CVDs.

6 Zusammenfassung

Herz-Kreislauf-Erkrankungen (CVD) wie Arrhythmien verursachen in Europa und weltweit immense gesundheitliche und wirtschaftliche Belastungen und sind Todesursache Nummer eins weltweit. Mitochondrien haben sich als Regulatoren der Herzrhythmik erwiesen, aber ihr Potenzial, als therapeutische Ziele gegen CVDs zu dienen, wurde bislang nicht weiter untersucht. Erst kürzlich wurde die synthetische Verbindung efsevin als potenter Modulator von Herzrhythmusstörung und zur Unterdrückung von Arrhythmien in einem Zebrafisch Model identifiziert. Die Effekte lassen sich auf eine Modulierung des spannungsabhängigen Anionen-Kanal 2 (VDAC2) zurückführen, einem porenbildenden Kanal in der äußeren mitochondrialen Membran (OMM). VDAC2 ermöglicht den Transport einer Vielzahl von Metaboliten und Ionen, einschließlich Ca^{2+}, durch das OMM und kann so regulierend wirken. Sein Potenzial, den Ca^{2+} Transport in den Mitochondrien direkt zu modulieren, war jedoch aufgrund seiner Porengröße fraglich.

In dieser Arbeit wurde die Wirkungsweise von Efsevin charakterisiert. Dabei konnten sowohl der anti-arrhythmische Effekt von efsevin gezeigt werden, als auch eine erhöhte mitochondriale-Ca^{2+} (mt-Ca^{2+}) Aufnahme als potentieller Mechanismus zur Behandlung von Arrhythmien etabliert werden. In einem Kardiomyozyten-Zellmodell konnte ich nachweisen, dass Efsevin zu einer erhöhten schnellen Ca^{2+} -Aufnahme in die Mitochondrien führt. Zusätzlich konnte gezeigt werden, dass in frisch isolierten RyR2R4496C/WT-Kardiomyozyten die erhöhte mt-Ca^{2+}-Aufnahme einen anti-arrhythmischen Effekt hat.

In einer zweiten Arbeit wurde die Efsevin-VDAC2-Interaktion biophysikalisch beschrieben. Dabei konnte gezeigt werden, dass Efsevin die Öffnungswahrscheinlichkeit von VDAC2 moduliert und den Kanal in einen kationenselektiven geschlossenen Zustand versetzt. Mit Hilfe von molekularem Liganden-Protein-„Docking“ wurde die Bindungsstelle von Efsevin an der Innenwand des Kanals, angrenzend an die N-terminale α-Helix identifiziert. Die Bindungsstelle wird durch die Aminosäuren N207, K237 und N238 gebildet. Der Austausch dieser drei Aminosäuren gegen Alanine führte zu einer Aufhebung der Efsevin-Sensitivität des Kanals. Dieser Effekt konnte auch in kultivierten murinen Kardiomyozyten in denen entweder Wildtyp zVDAC2 oder die Efsevin-insensitive zVDAC2^{AAA}-Mutante überexprimiert waren, gezeigt werden. Beide Kanäle, Wildtyp-zVDAC2 und die zVDAC2^{AAA}-Mutante, stellten die Aufnahme von

mitochondrialem Ca^{2+} in diesen Zellen wieder her. Jedoch konnte nur bei Wildtyp-zVDAC2 eine gesteigerte mitochondriale Ca^{2+}-Aufnahme durch Efsevin gemessen werden.

Zusammenfassend lässt sich sagen, dass in dieser Arbeit die pharmakologische Modulation der schnellen mitochondrialen Ca^{2+}-Aufnahme als Ansatz zur Behandlung von Arrhythmien etabliert wurde. Die Entschlüsselung der direkten Interaktion zwischen Efsevin und zVDAC2 zeigt neue Einblicke in die Funktionsweise von Kardiomyozyten und bildet die Grundlage für das computergestützte Design optimierter Substanzen, die in der Forschung und letztlich als Therapeutika für CVDs dienen könnten.[46]

7 References

1. Benjamin EJ, Virani SS, Callaway CW, et al. Heart disease and stroke statistics - 2018 update: A report from the American Heart Association. *Circulation*. 2018. doi:10.1161/CIR.0000000000000558

2. Wilkins E, Wilson I, Wickramasinghe K, et al. European Cardiovascular Disease Statistics 2017 edition. *Eur Hear Network, Brussels*. 2017. doi:978-2-9537898-1-2

3. WHO. World Health Oranization. https://www.who.int/news-room/fact-sheets/detail/cardiovascular-diseases-(cvds). Published 2016. Accessed January 6, 2020.

4. Ehn heart. No Title. http://www.ehnheart.org/cvd-statistics/cvd-statistics-2017.html. Published 2017. Accessed January 6, 2020.

5. Mehra R. Global public health problem of sudden cardiac death. *J Electrocardiol*. 2007. doi:10.1016/j.jelectrocard.2007.06.023

6. Mankad P, Kalahasty G. Antiarrhythmic Drugs: Risks and Benefits. *Med Clin North Am*. 2019;103(5):821-834. doi:10.1016/j.mcna.2019.05.004

7. Tse G. Mechanisms of cardiac arrhythmias. *J Arrhythmia*. 2016. doi:10.1016/j.joa.2015.11.003

8. Bers DM. Cardiac excitation-contraction coupling. *Nature*. 2002;415(6868):198-205. doi:10.1038/415198a

9. Landstrom AP, Dobrev D, Wehrens XHT. Calcium Signaling and Cardiac Arrhythmias. *Circ Res*. 2017;120(12):1969-1993. doi:10.1161/CIRCRESAHA.117.310083

10. Bootman MD, Higazi DR, Coombes S, Roderick HL. Calcium signalling during excitation-contraction coupling in mammalian atrial myocytes. *J Cell Sci*. 2006;119(19):3915-3925. doi:10.1242/jcs.03223

11. Williams GSB, Smith GD, Sobie EA, Jafri MS. Models of cardiac excitation-contraction coupling in ventricular myocytes. *Math Biosci*. 2010;226(1):1-15. doi:10.1016/j.mbs.2010.03.005

12. Endo M, Tanaka M, Ogawa Y. Calcium Induced release of calcium from the

Sarcoplasmic Reticulum of Skinned Skeletal Muscle Fibres. *Nature*. 1970. doi:10.1038/228034a0

13. Beuckelmann DJ, Wier WG. Mechanism of release of calcium from sarcoplasmic reticulum of guinea-pig cardiac cells. *J Physiol*. 1988. doi:10.1113/jphysiol.1988.sp017331

14. Jafri MS, Ullah A, Hoang-Trong T. Calcium sparks in the heart: dynamics and regulation. *Res Rep Biol*. 2015;6:203. doi:10.2147/rrb.s61495

15. Barth E, Stämmler G, Speiser B, Schaper J. Ultrastructural quantitation of mitochondria and myofilaments in cardiac muscle from 10 different animal species including man. *J Mol Cell Cardiol*. 1992. doi:10.1016/0022-2828(92)93381-S

16. Kim H -D, Kim CH, Rah B -J, Chung H -I, Shim T -S. Quantitative study on the relation between structural and functional properties of the hearts from three different mammals. *Anat Rec*. 1994. doi:10.1002/ar.1092380206

17. De la Fuente S, Sheu SS. SR-mitochondria communication in adult cardiomyocytes: A close relationship where the Ca 2+ has a lot to say. *Arch Biochem Biophys*. 2019;663:259-268. doi:10.1016/j.abb.2019.01.026

18. Rossini M, Filadi R. Sarcoplasmic Reticulum-Mitochondria Kissing in Cardiomyocytes: Ca2+, ATP, and Undisclosed Secrets. *Front Cell Dev Biol*. 2020;8:532. doi:10.3389/fcell.2020.00532

19. De Kroon AIPM, Dolis D, Mayer A, Lill R, De Kruijff B. Phospholipid composition of highly purified mitochondrial outer membranes of rat liver and Neurospora crassa. Is cardiolipin present in the mitochondrial outer membrane? *Biochim Biophys Acta - Biomembr*. 1997. doi:10.1016/S0005-2736(96)00240-4

20. Pape H-C 1956-, Kurtz A 1955-, Silbernagl S 1939-, et al. *Physiologie*. https://www.thieme.de/shop/Physiologie/Pape-Kurtz-Silbernagl-Physiologie-9783132423879/p/000000000210930108. Accessed March 13, 2019.

21. Báthori G, Csordás G, Garcia-Perez C, Davies E, Hajnóczky G. Ca2+-dependent control of the permeability properties of the mitochondrial outer membrane and voltage-dependent anion-selective channel (VDAC). *J Biol Chem*. 2006;281(25):17347-17358. doi:10.1074/jbc.M600906200

22. Seguchi H, Ritter M, Shizukuishi M, et al. Propagation of Ca2+ release in cardiac

myocytes: Role of mitochondria. *Cell Calcium*. 2005. doi:10.1016/j.ceca.2005.03.004

23. Zhao Z, Gordan R, Wen H, Fefelova N, Zang WJ, Xie LH. Modulation of intracellular calcium waves and triggered activities by mitochondrial Ca flux in mouse cardiomyocytes. *PLoS One*. 2013. doi:10.1371/journal.pone.0080574

24. Gambardella J, Sorriento D, Ciccarelli M, et al. Functional role of mitochondria in arrhythmogenesis. In: *Advances in Experimental Medicine and Biology*. Vol 982. Springer New York LLC; 2017:191-202. doi:10.1007/978-3-319-55330-6_10

25. Yang K-C, Bonini MG, Dudley SC. Mitochondria and arrhythmias. *Free Radic Biol Med*. 2014;71:351-361. doi:10.1016/j.freeradbiomed.2014.03.033

26. Shimizu H, Schredelseker J, Huang J, et al. Mitochondrial Ca(2+) uptake by the voltage-dependent anion channel 2 regulates cardiac rhythmicity. *Elife*. 2015;4. doi:10.7554/eLife.04801

27. Min CK, Yeom DR, Lee K-E, et al. Coupling of ryanodine receptor 2 and voltage-dependent anion channel 2 is essential for Ca^{2}+ transfer from the sarcoplasmic reticulum to the mitochondria in the heart. *Biochem J*. 2012;447(3):371-379. doi:10.1042/BJ20120705

28. Xu Z, Zhang D, He X, Huang Y, Shao H. Transport of Calcium Ions into Mitochondria. *Curr Genomics*. 2016. doi:10.2174/1389202917666160202215748

29. Sander P, Gudermann T, Schredelseker J. A calcium guard in the outer membrane: Is vdac a regulated gatekeeper of mitochondrial calcium uptake? *Int J Mol Sci*. 2021;22(2):1-18. doi:10.3390/ijms22020946

30. Ebert AM, Hume GL, Warren KS, et al. Calcium extrusion is critical for cardiac morphogenesis and rhythm in embryonic zebrafish hearts. *Proc Natl Acad Sci U S A*. 2005;102(49):17705-17710. doi:10.1073/pnas.0502683102

31. Shu X, Philipson KD, Choi J, et al. Mutation in sodium-calcium exchanger 1 (NCX1) causes cardiac fibrillation in zebrafish. *Proc Natl Acad Sci*. 2005. doi:10.1073/pnas.0502679102

32. Schein SJ, Colombini M, Finkelstein A. Reconstitution in planar lipid bilayers of a voltage-dependent anion-selective channel obtained from paramecium mitochondria. *J Membr Biol*. 1976. doi:10.1007/BF01869662

33. Dolder M, Zeth K, Tittmann P, Gross H, Welte W, Wallimann T. Crystallization of the human, mitochondrial voltage-dependent anion- selective channel in the presence of phospolipids. *J Struct Biol*. 1999. doi:10.1006/jsbi.1999.4141

34. Schredelseker J, Paz A, López CJ, et al. High Resolution Structure and Double Electron-Electron Resonance of the Zebrafish Voltage-dependent Anion Channel 2 Reveal an Oligomeric Population. *J Biol Chem*. 2014;289(18):12566-12577. doi:10.1074/jbc.M113.497438

35. Colombini M, Blachly-Dyson E, Forte M. VDAC, a Channel in the Outer Mitochondrial Membrane. In: *Ion Channels*. ; 2013. doi:10.1007/978-1-4899-1775-1_5

36. Becker S, Meins T, Villinger S, et al. Structure of the human voltage-dependent anion channel. *Proc Natl Acad Sci*. 2008. doi:10.1073/pnas.0808115105

37. Hiller S, Garces RG, Malia TJ, Orekhov VY, Colombini M, Wagner G. Solution structure of the integral human membrane protein VDAC-1 in detergent micelles. *Science (80-)*. 2008. doi:10.1126/science.1161302

38. Gincel D, Zaid H, Shoshan-Barmatz V. Calcium binding and translocation by the voltage-dependent anion channel: A possible regulatory mechanism in mitochondrial function. *Biochem J*. 2001;358(1):147-155. doi:10.1042/0264-6021:3580147

39. Shoshan-Barmatz V, De S, Meir A. The mitochondrial voltage-dependent anion channel 1, Ca2+ transport, apoptosis, and their regulation. *Front Oncol*. 2017;7(APR). doi:10.3389/fonc.2017.00060

40. Naghdi S, Hajnóczky G. VDAC2-specific cellular functions and the underlying structure. *Biochim Biophys Acta*. 2016;1863(10):2503-2514. doi:10.1016/j.bbamcr.2016.04.020

41. Wu S, Sampson MJ, Decker WK, Craigen WJ. Each mammalian mitochondrial outer membrane porin protein is dispensable: Effects on cellular respiration. *Biochim Biophys Acta - Mol Cell Res*. 1999. doi:10.1016/S0167-4889(99)00120-2

42. Ujwal R, Cascio D, Colletier J-P, et al. The crystal structure of mouse VDAC1 at 2.3 A resolution reveals mechanistic insights into metabolite gating. *Proc Natl Acad Sci*. 2008. doi:10.1073/pnas.0809634105

43. Colombini M. VDAC structure, selectivity, and dynamics. *Biochim Biophys Acta - Biomembr*. 2012. doi:10.1016/j.bbamem.2011.12.026

44. Briones R, Weichbrodt C, Paltrinieri L, et al. Voltage Dependence of Conformational Dynamics and Subconducting States of VDAC-1. *Biophys J*. 2016;111(6):1223-1234. doi:10.1016/j.bpj.2016.08.007

45. Levadny V, Colombini M, Li XX, Aguilella VM. Electrostatics explains the shift in VDAC gating with salt activity gradient. *Biophys J*. 2002;82(4):1773-1783. doi:10.1016/S0006-3495(02)75528-8

46. Sander P, Feng M, Schweitzer MK, et al. Approved drugs ezetimibe and disulfiram enhance mitochondrial Ca2+ uptake and suppress cardiac arrhythmogenesis. *Br J Pharmacol*. 2021;178(22):4518-4532. doi:10.1111/bph.15630

8 Paper 1: Suppression of Arrhythmia by Enhancing Mitochondrial Ca^{2+} Uptake in Catecholaminergic Ventricular Tachycardia Models

JACC: BASIC TO TRANSLATIONAL SCIENCE
VOL. 2, NO. 6, 2017
ISSN 2452-302X
https://doi.org/10.1016/j.jacbts.2017.06.008

PRECLINICAL RESEARCH

Suppression of Arrhythmia by Enhancing Mitochondrial Ca^{2+} Uptake in Catecholaminergic Ventricular Tachycardia Models

Maria K. Schweitzer, MSc,[a] Fabiola Wilting, MSc,[a] Simon Sedej, PhD,[b] Lisa Dreizehnter, PhD,[c] Nathan J. Dupper, BSc,[d] Qinghai Tian, PhD,[e] Alessandra Moretti, PhD,[c,f] Ilaria My, MD,[c] Ohyun Kwon, PhD,[d] Silvia G. Priori, MD, PhD,[g,h] Karl-Ludwig Laugwitz, MD,[c,f] Ursula Storch, PhD,[a] Peter Lipp, PhD,[e] Andreas Breit, PhD,[a] Michael Mederos y Schnitzler, PhD,[a,f] Thomas Gudermann, MD,[a,f] Johann Schredelseker, PhD[a]

VISUAL ABSTRACT

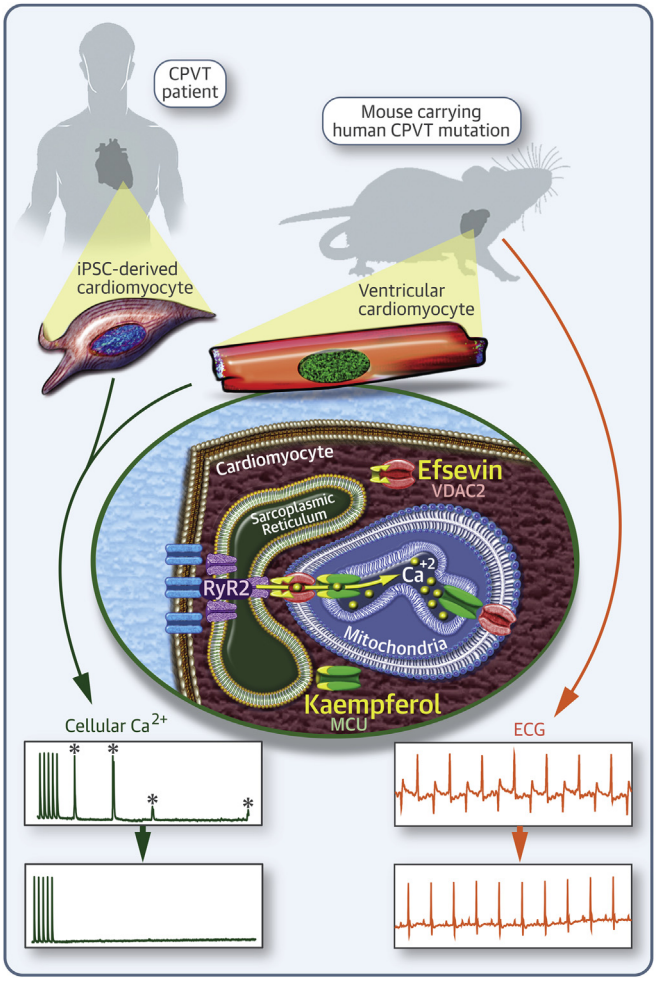

Schweitzer, M.K. et al. J Am Coll Cardiol Basic Trans Science. 2017;2(6):737–47.

HIGHLIGHTS

- Fast transfer of Ca^{2+} from the sarcoplasmic reticulum into mitochondria in cardiomyocytes can be enhanced by the MiCUps efsevin, targeting the VDAC2, and kaempferol, targeting the MCU.
- Enhancing sarcoplasmic reticulum-to-mitochondria Ca^{2+} transfer with MiCUps suppresses arrhythmogenic Ca^{2+} events and spontaneous action potentials in cardiomyocytes from a mouse model of CPVT.
- In vivo treatment of CPVT mice with MiCUps reduces episodes of ventricular tachycardia after adrenergic stimulation.
- In induced pluripotent stem cell-derived cardiomyocytes from a CPVT patient, both MiCUps reduce arrhythmogenic Ca^{2+} events.
- Our data establish fast mitochondrial Ca^{2+} uptake as a promising candidate structure for pharmacological treatment of human cardiac arrhythmia.

ABBREVIATIONS AND ACRONYMS

CPVT = catecholaminergic polymorphic ventricular tachycardia

epi/caff = epinephrine/caffeine

iPSC = induced pluripotent stem cell

ISO = isoproterenol

MCU = mitochondrial calcium uniporter

MiCUp = mitochondrial calcium uptake enhancer

RyR2 = ryanodine receptor type 2

SR = sarcoplasmic reticulum

VDAC2 = voltage-dependent anion channel type 2

WT = wild type

SUMMARY

Cardiovascular disease-related deaths frequently arise from arrhythmias, but treatment options are limited due to perilous side effects of commonly used antiarrhythmic drugs. Cardiac rhythmicity strongly depends on cardiomyocyte Ca^{2+} handling and prevalent cardiac diseases are causally associated with perturbations in intracellular Ca^{2+} handling. Therefore, intracellular Ca^{2+} transporters are lead candidate structures for novel and safer antiarrhythmic therapies. Mitochondria and mitochondrial Ca^{2+} transport proteins are important regulators of cardiac Ca^{2+} handling. Here, the authors evaluated the potential of pharmacological activation of mitochondrial Ca^{2+} uptake for the treatment of cardiac arrhythmia. To this aim, the authors tested substances that enhance mitochondrial Ca^{2+} uptake for their ability to suppress arrhythmia in a murine model for ryanodine receptor 2 (RyR2)-mediated catecholaminergic polymorphic ventricular tachycardia (CPVT) in vitro and in vivo and in induced pluripotent stem cell-derived cardiomyocytes from a CPVT patient. In freshly isolated cardiomyocytes of $RyR2^{R4496C/WT}$ mice efsevin, a synthetic agonist of the voltage-dependent anion channel 2 (VDAC2) in the outer mitochondrial membrane, prevented the formation of diastolic Ca^{2+} waves and spontaneous action potentials. The antiarrhythmic effect of efsevin was abolished by blockade of the mitochondrial Ca^{2+} uniporter (MCU), but could be reproduced using the natural MCU activator kaempferol. Both mitochondrial Ca^{2+} uptake enhancers (MiCUps), efsevin and kaempferol, significantly reduced episodes of stress-induced ventricular tachycardia in $RyR2^{R4496C/WT}$ mice in vivo and abolished diastolic, arrhythmogenic Ca^{2+} events in human iPSC-derived cardiomyocytes. These results highlight an immediate potential of enhanced mitochondrial Ca^{2+} uptake to suppress arrhythmogenic events in experimental models of CPVT and establish MiCUps as promising pharmacological tools for the treatment and prevention of Ca^{2+}-triggered arrhythmias such as CPVT. (J Am Coll Cardiol Basic Trans Science 2017;2:737–47)

Cardiovascular diseases remain the leading cause of death worldwide (1). Approximately one-half of all cardiovascular deaths are attributed to severe cardiac arrhythmia (2). Cardiac rhythmicity critically depends on precisely regulated Ca^{2+} oscillations in cardiomyocytes (3), and cardiac arrhythmia is frequently associated with perturbations of cellular Ca^{2+} handling (4,5). Most currently used antiarrhythmic drugs target receptors and channels in the cell membrane (sarcolemma) to block the propagation of arrhythmic events along the myocardium but do not restore defective intracellular Ca^{2+} handling. Due to their modulatory effects on the cardiac action potential, these drugs often show pro-arrhythmic side effects. Therefore, intracellular Ca^{2+} transporters are candidate structures for novel and safer antiarrhythmic therapies.

Mitochondria occupy approximately 30% of the cardiomyocyte volume (6,7) and closely interact with the sarcoplasmic reticulum (SR) to absorb Ca^{2+}, which is released from the SR into the cytosol through cardiac ryanodine receptors (RyR2) (8,9). For that, mitochondria are equipped with a regulated network of Ca^{2+} transporters. While the mitochondrial calcium

From the [a]Walther Straub Institute of Pharmacology and Toxicology, Ludwig-Maximilians-Universität München, Munich, Germany; [b]Department of Cardiology, Medical University of Graz, Graz, Austria; [c]Department of Medicine (Cardiology), Klinikum rechts der Isar, Technische Universität München, Munich, Germany; [d]Department of Chemistry and Biochemistry, University of California Los Angeles, Los Angeles, California; [e]Institute for Molecular Cell Biology, University Medical Center, Saarland University, Homburg/Saar, Germany; [f]Deutsches Zentrum für Herz-Kreislauf-Forschung, Partner Site Munich Heart Alliance, Munich, Germany; [g]Molecular Cardiology, Istituto di ricovero e cura a carattere scientifico (IRCCS) Salvatore Maugeri Foundation, Pavia, Italy; and the [h]Department of Molecular Medicine, University of Pavia, Pavia, Italy. Supported by Deutsche Forschungsgemeinschaft (DFG), Bonn, Germany (SCHR 1471/1-1 to Dr. Schredelseker; TRR152 to Drs. Gudermann, Lipp, Moretti, and Laugwitz), the Friedrich-Baur-Stiftung, Munich, Germany (to Dr. Schredelseker), and U.S. National Institutes of Health (R01GM071779 to Dr. Kwon). Dr. Sedej is supported by the Austrian Science Fund FWF, Vienna, Austria (P27637-B28). Dr. Priori has received research support from Boston Scientific; and is a member of the advisory boards for General Electric and Audentes. All other authors have reported that they have no relationships relevant to the contents of this paper to disclose.
All authors attest they are in compliance with human studies committees and animal welfare regulations of the authors' institutions and Food and Drug Administration guidelines, including patient consent where appropriate. For more information, visit the *JACC: Basic to Translational Science* author instructions page.

Manuscript received April 10, 2017; revised manuscript received June 26, 2017, accepted June 27, 2017.

uniporter (MCU) has been identified as the main route for Ca^{2+} import in the inner mitochondrial membrane (10–12), the voltage-dependent anion channel 2 (VDAC2) in the outer mitochondrial membrane has only recently been shown to be a major part of the Ca^{2+} transport route from the SR into mitochondria (13–15). In addition to the 2 pore-forming channels, the mitochondrial Ca^{2+} uptake complex is regulated by several auxiliary subunits such as the essential MCU regulator EMRE or the mitochondrial Ca^{2+} uptake proteins MICU1 and -2 (16,17). While it is generally accepted that a slow and moderate rise of mitochondrial Ca^{2+} triggers enhanced energy production under higher workload (18), the immediate role of mitochondria in shaping cellular Ca^{2+} signals on a beat-to-beat level remains a matter of debate (19,20). Mitochondria have been demonstrated to be regulators of cardiac rhythmicity (21,22), but their potential to serve as therapeutic targets has not been evaluated so far. The synthetic compound efsevin has been newly identified to activate VDAC2 and to enhance mitochondrial Ca^{2+} uptake (15). Using efsevin, we demonstrated that cardiac rhythmicity in zebrafish embryos can be critically modulated by enhancing mitochondrial Ca^{2+} uptake (15).

This study evaluated the translational potential of pharmacological activation of mitochondrial Ca^{2+} uptake for the prevention and treatment of cardiac arrhythmia. To this end, we used 2 models of catecholaminergic polymorphic ventricular tachycardia (CPVT), exemplifying a Ca^{2+}-triggered arrhythmia. CPVT manifests in early adolescence and is characterized by episodes of life-threatening ventricular tachycardia upon catecholaminergic stimulation after physical exercise or emotional stress. The $RyR2^{R4496C/WT}$ mouse harbors an R4496C mutation in the SR Ca^{2+} release channel RyR2, homologous to the human R4497C mutation, which is associated with CPVT (23) and displays a CPVT phenotype (24). We show that activating mitochondrial Ca^{2+} uptake suppresses arrhythmia in $RyR2^{R4496C/WT}$ cardiomyocytes in vitro and in $RyR^{R4496C/WT}$ mice in vivo. Finally, we demonstrate that activating mitochondrial Ca^{2+} uptake is likewise efficient in blocking arrhythmogenesis in induced pluripotent stem cell (iPSC)-derived cardiomyocytes from a CPVT patient heterozygous for a different RyR2 mutation ($RyR2^{S406L}$).

METHODS

ISOLATION OF CARDIOMYOCYTES. Isolation of ventricular cardiomyocytes from heterozygous knock-in $RyR2^{R4496C/WT}$ mice (24) was performed using a Langendorff perfusion-based enzymatic digestion protocol (25) with minor modifications. Only excitable, rod-shaped, quiescent cells were used for experiments.

HUMAN iPSC-BASED MODEL. iPSCs from a skin biopsy from a CPVT patient carrying the $RyR2^{S406L/WT}$ mutation and from a healthy donor were differentiated into spontaneously beating explants (26,27) and enzymatically dissociated into single cardiomyocytes.

Ca^{2+} IMAGING. Ca^{2+} transients, spontaneous diastolic Ca^{2+} waves, and Ca^{2+} sparks were measured in cardiomyocytes loaded with Fluo-4 acetoxymethyl ester (AM) (Thermo Fisher Scientific, Darmstadt, Germany), using confocal microscopy in line scan mode. Cells were paced by extracellular electrodes at 0.5 Hz.

ELECTROPHYSIOLOGY. Action potentials were recorded in current clamp mode, using the perforated patch-clamp technique. Cells were paced by repetitive, depolarizing intracellular current injections at 0.5 Hz, followed by a 60-s pause to detect potentially proarrhythmic events during this diastolic phase.

cAMP ACCUMULATION ASSAY. For evaluation of intracellular cAMP levels, cardiomyocytes were labeled with ^{3}H-labeled adenine to measure accumulation of [^{3}H]cAMP over 15 min.

IN VIVO ARRHYTHMIA TESTING. Drugs were administered to $RyR2^{R4496C/WT}$ mice 8 to 12 weeks of age through osmotic minipumps, and subsequently, electrocardiography recordings were performed under light isoflurane anesthesia, to monitor ventricular tachycardia after bolus injection of epinephrine/caffeine (epi/caff). All animal procedures were performed in accordance with national and European ethical regulations (directive 2010/63/EU) and approved by the responsible government agency (BMWFW-66.010/0012-WF/V/3b/2015).

MITOCHONDRIAL Ca^{2+} UPTAKE. Mitochondrial Ca^{2+} uptake in response to 10 mM caffeine to open RyR2 was measured in Rhod-2 AM-loaded permeabilized HL-1 cardiomyocytes (28) on a fluorescence 96-well plate reader. The Ca^{2+} chelator 1,2-*bis*(*o*-aminophenoxy) ethane-*N*,*N*,*N*′,*N*′-tetraacetic acid (BAPTA) (1 mM) was used to restrict Ca^{2+} to the low micrometer range around RyR clusters (8,29).

STATISTICAL ANALYSIS. Data are mean ± standard error of the mean. Normality of data was determined by Shapiro-Wilk test, and respective tests for statistical significance were conducted as indicated. Post hoc tests were Dunn's test for Kruskal-Wallis tests and Tukey's multiple comparisons test for ANOVA. Significance for contingency tables was calculated using Fisher's exact test.

FIGURE 1 Efsevin Reduces Diastolic Ca^{2+} Waves and Spontaneous Action Potentials in $RyR2^{R4496C/WT}$ Cardiomyocytes

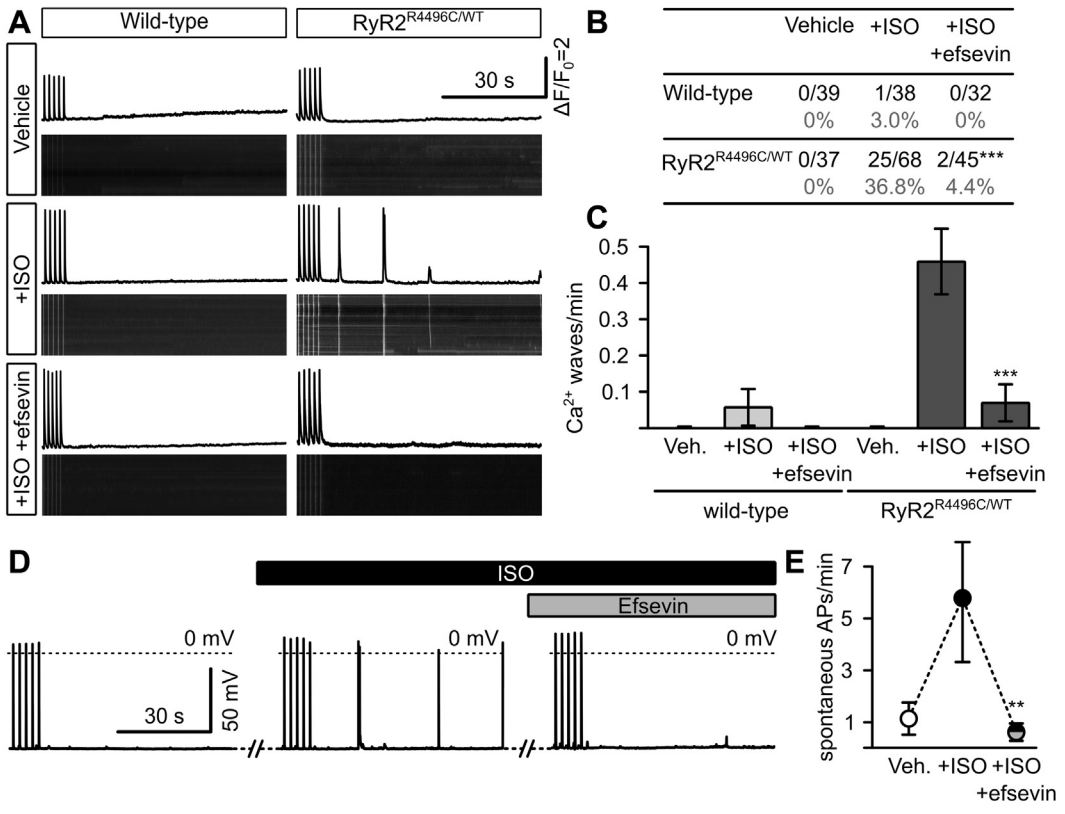

(A) Confocal line scans across the long axis of freshly isolated cardiomyocytes from wild-type and $RyR2^{R4496C/WT}$ mice loaded with Fluo-4 AM to measure intracellular Ca^{2+}. Images show line scans, and graphs depict fluorescence intensity plots. Cells were stimulated at 0.5 Hz for 30 s to reach steady state conditions (last 5 Ca^{2+} transients are shown) before pulsing was stopped and the diastolic phase was recorded for 90 s to screen for spontaneous diastolic Ca^{2+} waves. **(B)** While wild-type cells never showed a significant frequency of spontaneous diastolic Ca^{2+} waves, 25 of 68 $RyR2^{R4496C/WT}$ cardiomyocytes showed waves, which could be significantly reduced to 2 of 45 cells ($p < 0.001$, Fisher's exact test) by addition of 15 μM efsevin. **(C)** Average number of Ca^{2+} waves per minute was significantly enhanced from 0 in vehicle-treated $RyR2^{R4496C/WT}$ cardiomyocytes to 0.46 ± 0.09 waves/min in cells treated with 1 μM ISO ($p < 0.001$, Kruskal-Wallis test). Addition of 15 μM efsevin reduced the number of waves/minute to 0.07 ± 0.05 to levels indistinguishable from untreated cells ($p = 0.578$). **(D)** Patch clamp recordings from $RyR2^{R4496C/WT}$ cardiomyocytes showed an increase in spontaneous action potentials after superfusion with ISO, which were eliminated by addition of 15 μM efsevin. **(E)** Quantitative analysis of patch clamp recordings revealed a significant increase of spontaneous diastolic action potentials (APs) from 1.12 ± 0.62 APs/min under vehicle (Veh.) to 5.76 ± 2.45 APs/min after superfusion with ISO ($p = 0.018$, Friedman test, $n = 15$) and a significant reduction to 0.58 ± 0.34 APs/min when simultaneously treated with ISO and efsevin ($p = 0.011$). **$p < 0.01$; ***$p < 0.001$. ISO = isoproterenol.

Please see the detailed Methods in the Supplemental Appendix.

RESULTS

EFSEVIN REDUCES ARRHYTHMOGENIC Ca^{2+} WAVES IN $RyR2^{R4496C/WT}$ CARDIOMYOCYTES. The triggers for arrhythmia originating from imbalanced cellular Ca^{2+} homeostasis, such as CPVT, are intracellular Ca^{2+} waves during diastole, which arise from an increased SR Ca^{2+} leak through RyR2 (30). We therefore recorded diastolic Ca^{2+} waves in freshly isolated ventricular cardiomyocytes from $RyR2^{R4496C/WT}$ mice and their wild-type (WT) littermates. Under control conditions (vehicle), neither WT cardiomyocytes nor $RyR2^{R4496C/WT}$ cells showed spontaneous Ca^{2+} waves within 90 s after preceding electrical stimulation at 0.5 Hz. However, unlike WT cells, $RyR2^{R4496C/WT}$ cardiomyocytes displayed pronounced spontaneous, diastolic Ca^{2+} waves after stimulation with the catecholamine isoproterenol (ISO) (Figures 1A to 1C). Strikingly, application of 15 μM efsevin significantly reduced the number of cells displaying such Ca^{2+} waves and the average number of Ca^{2+} waves per

FIGURE 2 Efsevin Does Not Affect Beta-Adrenergic Stimulation in $RyR2^{R4496C/WT}$ Cardiomyocytes

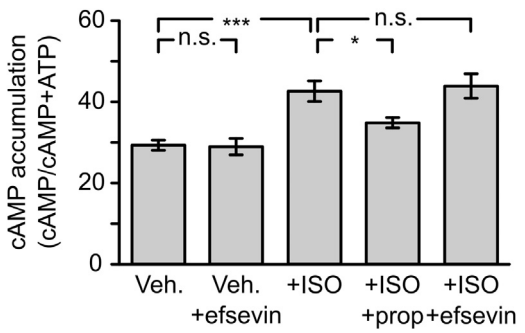

cAMP accumulation in freshly isolated $RyR2^{R4496C/WT}$ cardiomyocytes was measured in response to different stimuli. Efsevin had no effect on cellular cAMP levels ($p > 0.999$, Kruskal-Wallis test), whereas ISO induced a significant increase in cellular cAMP ($p < 0.001$). This increase could be blocked using the beta-adrenoreceptor blocker propranolol (prop) ($p = 0.036$), although efsevin had no effect on the ISO-induced increase in cellular cAMP ($p = 0.999$), indicating that efsevin neither activates nor blocks the beta-adrenergic system in cardiomyocytes. *$p < 0.05$; ***$p < 0.001$. Abbreviations as in Figure 1.

minute in $RyR2^{R4496C/WT}$ cardiomyocytes to levels of unstimulated $RyR2^{R4496C/WT}$ cells and WT cells. Notably, in contrast to previous data from unstimulated cells (15), efsevin did not exert any significant effects on the amplitude and kinetics of electrically evoked Ca^{2+} transients under ISO stimulation (Supplemental Figure 1).

EFSEVIN REDUCES SPONTANEOUS ACTION POTENTIALS IN $RyR2^{R4496C/WT}$ CARDIOMYOCYTES. Cardiac arrhythmia is triggered when Ca^{2+} waves activate the sarcolemmal sodium-calcium exchanger, leading to a transient depolarizing sodium inward current and finally spontaneous action potentials (31), which can propagate along the myocardium. Hence, we recorded spontaneous action potentials in patch-clamped $RyR2^{R4496C/WT}$ cardiomyocytes. We observed a significant increase in the frequency of spontaneous action potentials after cells were superfused with 1 μM ISO. Subsequent treatment with 15 μM efsevin effectively reduced these spontaneous depolarizations to baseline levels (**Figures 1D and 1E**). Notably, efsevin did not exert any effects on the resting membrane potential and amplitude of electrically evoked action potentials under ISO stimulation but caused a significant change of the repolarization phase (Supplemental Figure 1), namely a prolongation of the action potential duration at 50% repolarization (APD50) but not at 90% repolarization (APD90). To evaluate whether this effect seen on the fast, inactivating mouse action potential (32) could lead to QT prolongation in human cells, we recorded action potentials from human iPSC-derived cardiomyocytes in the presence of efsevin and found no changes in APD50 and APD90 compared to vehicle-treated cells (Supplemental Figures 2A and 2B). Furthermore, efsevin did not inhibit hERG channel activity in a heterologous expression system at relevant concentrations (Supplemental Figure 2C).

THE ANTIARRHYTHMIC EFFECT OF EFSEVIN IS MEDIATED BY MITOCHONDRIAL Ca^{2+} UPTAKE. We next investigated the mechanism of efsevin's antiarrhythmic effect. To exclude the possibility that efsevin directly blocks catecholaminergic stimulation by ISO, we measured cAMP accumulation in efsevin-treated $RyR2^{R4496C/WT}$ cardiomyocytes. Stimulation by ISO induced a significant increase in cellular cAMP, which was blocked by the beta-adrenoreceptor blocker propranolol. Addition of efsevin alone did not increase or decrease cellular cAMP concentrations, and addition of efsevin to stimulated cells had no effect on the ISO-induced cAMP increase, indicating that efsevin does not influence beta-adrenergic signaling in cardiomyocytes (**Figure 2**).

Efsevin significantly enhanced transfer of Ca^{2+} from the SR into mitochondria in a Ca^{2+} uptake assay in permeabilized cultured HL-1 cardiomyocytes. Mitochondrial Ca^{2+} was measured after addition of 10 mM caffeine to open RyR2s in the presence of the Ca^{2+} chelator BAPTA to restrict Ca^{2+} released from RyRs to the low micrometer range around RyR clusters (8,29) (**Figure 3A**). The efsevin-sensitive Ca^{2+} transfer between the SR and mitochondria was blocked by addition of the MCU blocker ruthenium red. To test whether the enhanced SR-mitochondria Ca^{2+} transfer was directly responsible for the reduction of diastolic Ca^{2+} wave frequency in $RyR2^{R4496C/WT}$ cardiomyocytes, we assessed whether blocking of mitochondrial Ca^{2+} uptake abolished the antiarrhythmic effect of efsevin. We measured catecholamine-induced Ca^{2+} waves in $RyR2^{R4496C/WT}$ myocytes under simultaneous blockade of mitochondrial Ca^{2+} uptake, using the MCU inhibitor Ru360 (**Figure 3B**). We observed a moderately higher Ca^{2+} wave frequency under all conditions, consistent with the idea that mitochondrial Ca^{2+} uptake prevents Ca^{2+} wave formation. Most strikingly, the ability of efsevin to suppress the ISO-induced increase in Ca^{2+} wave frequency was abolished in the presence of Ru360, indicating that the suppression of diastolic Ca^{2+} waves by efsevin is solely mediated by enhanced mitochondrial Ca^{2+} uptake.

FIGURE 3 Efsevin Acts Through Mitochondrial Ca^{2+} Uptake

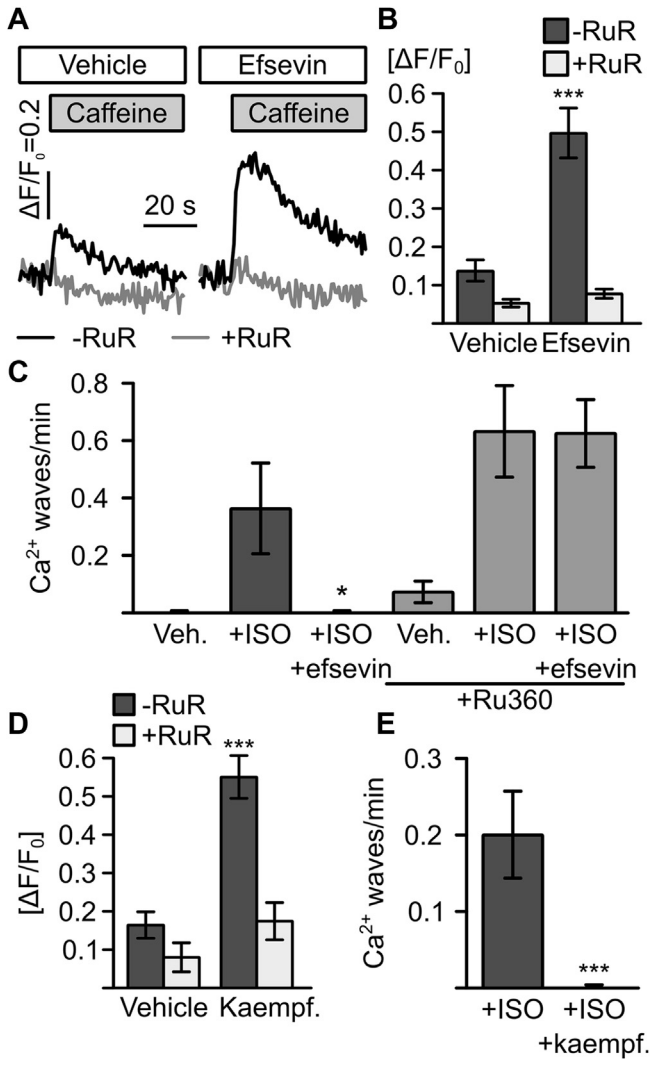

(A) Representative recordings of mitochondrial Ca^{2+} in permeabilized HL-1 cardiomyocytes. Superfusion with caffeine induced a rapid uptake of Ca^{2+} into mitochondria **(black trace)**, which was enhanced by 15 μM efsevin and blocked by 10 μM RuR **(gray trace)**. **(B)** Quantification of peak mitochondrial fluorescence showed a significant increase in mitochondrial Ca^{2+} uptake in cells treated with efsevin from $\Delta F/F_0 = 0.14 \pm 0.03$ ($n = 10$) to 0.50 ± 0.07 ($n = 19$, $p < 0.001$, ANOVA). **(C)** 15 μM efsevin reduces spontaneous propagating waves in $RyR2^{R4496C/WT}$ cardiomyocytes under ISO influence from 0.36 ± 0.16 waves/min ($n = 15$) to 0 **(black bars)** ($n = 21$, $p = 0.035$, Kruskal-Wallis test). In the presence of 8 μM of the mitochondrial Ca^{2+} uptake blocker Ru360, vehicle-treated cells showed 0.07 ± 0.04 waves/min ($n = 29$), which increased to 0.63 ± 0.16 under ISO influence ($n = 21$, $p < 0.001$) but could not be blocked with efsevin as shown by an indistinguishable value of 0.62 ± 0.12 waves/min under ISO influence together with efsevin **(gray bars)** ($n = 62$, $p = 0.354$ compared to that with ISO). **(D)** 10 μM of the MCU activator kaempferol significantly increased mitochondrial Ca^{2+} uptake after SR Ca^{2+} release from $\Delta F/F_0 = 0.16 \pm 0.04$ ($n = 9$) to 0.55 ± 0.05 ($n = 10$, $p < 0.001$, ANOVA) Ca^{2+} uptake was inhibited by 50 μM RuR **(gray bars)**. **(E)** Treatment of $RyR2^{R4496C/WT}$ cardiomyocytes with 10 μM kaempferol completely eliminated ISO-induced spontaneous diastolic Ca^{2+} waves from 0.19 ± 0.04 waves/min ($n = 49$) to 0 ($n = 45$; $p < 0.001$, Mann-Whitney *U* test). *$p < 0.05$; ***$p < 0.001$. $\Delta F/F_0$ = change in fluorescence over baseline fluorescence; MCU = mitochondrial Ca^{2+} uniporter; RuR = ruthenium red; SR = sarcoplasmic reticulum.

We next tested if enhancing mitochondrial Ca^{2+} uptake was a general pharmacological approach to suppress arrhythmogenic events or if it is limited to a specific effect of efsevin on VDAC2. To this purpose, we used another activator of mitochondrial Ca^{2+} uptake, the natural plant flavonoid kaempferol, which was reported to directly activate MCU in the inner mitochondrial membrane (33,34). Indeed, kaempferol increased SR-mitochondria Ca^{2+} transfer, comparable to efsevin (**Figure 3D**). To evaluate the antiarrhythmic potential of kaempferol, we measured diastolic Ca^{2+} waves in kaempferol-treated $RyR2^{R4496C/WT}$ cardiomyocytes under ISO to induce catecholaminergic stimulation. Strikingly, 10 μM kaempferol completely eliminated ISO-induced arrhythmogenic Ca^{2+} waves in $RyR2^{R4496C/WT}$ cardiomyocytes (**Figure 3E**).

It was previously reported that enhanced mitochondrial Ca^{2+} uptake in cardiomyocytes restricts diffusion of Ca^{2+} inside the cytosol (13) and thereby prevents propagation of cytosolic Ca^{2+} signals under conditions of Ca^{2+} overload (15). Because an enhanced RyR-mediated Ca^{2+} leak was reported to be the mechanism responsible for arrhythmogenesis in CPVT (35–37), we recorded Ca^{2+} sparks from $RyR2^{R4496C/WT}$ cardiomyocytes (**Figure 4**). We observed an increase in Ca^{2+} spark frequency and amplitude after treatment with ISO, consistent with previous work (36), thus explaining the enhanced Ca^{2+} wave frequency under catecholaminergic stimulation. Strikingly, the SR leak in cells treated with ISO together with efsevin was reduced compared to that in cells treated with ISO alone, as indicated by a decrease in Ca^{2+} spark frequency and amplitude. Also, we found removal of cytosolic Ca^{2+} was accelerated under efsevin stimulation, leading to a reduction of full width and full duration of Ca^{2+} sparks. Together, these effects explain the suppressive effect of efsevin on propagating Ca^{2+} waves.

MiCUps REDUCE EPISODES OF STRESS-INDUCED VENTRICULAR TACHYCARDIA IN VIVO. To assess the potency of both of the mitochondrial Ca^{2+} uptake enhancers (MiCUps), efsevin and kaempferol, to suppress arrhythmia in vivo, we administered efsevin and kaempferol to $RyR2^{R4496C/WT}$ mice, using implantable osmotic minipumps. All mice recovered well from surgery, and their behavior was grossly normal. Treated mice showed no signs of discomfort, stress, or abnormal behavior. After 3 days, efsevin and kaempferol showed no effect on electrocardiography (ECG) parameters such as the interval between atrial and ventricular depolarization (PR), the interval between ventricular depolarization and subsequent repolarization (QT), or conduction of ventricular

depolarization (QRS) and basal heart rate (Figures 5A and 5B). To activate their adrenergic response, we injected mice with a bolus of 2 mg/kg epinephrine and 120 mg/kg caffeine (epi/caff). The epi/caff injection induced a significant increase in heart rate in all 3 groups, but no differences were observed between vehicle-treated mice and mice treated with MiCUps. Most strikingly, both of the MiCUps significantly reduced episodes of bidirectional ventricular tachycardia under catecholaminergic stimulation. Injection of epi/caff provoked bidirectional ventricular tachycardia in all vehicle-treated control animals (n = 11) but only in 6 of 10 mice treated with efsevin and 6 of 11 mice treated with kaempferol (Figures 5D and 5E). Comparable results were obtained from mice treated with efsevin for 8 days (Supplemental Figure 3).

MiCUps REDUCE ARRHYTHMOGENIC Ca^{2+} WAVES IN iPSC-DERIVED CARDIOMYOCYTES FROM A CPVT PATIENT. In order to evaluate the translational potential of MiCUps for the treatment of CPVT, we used a human cell-based arrhythmia model for CPVT. Human iPSC-derived cardiomyocytes from a CPVT patient heterozygous for the $RyR2^{S406L}$ mutation associated with CPVT (26) were used to record arrhythmogenic Ca^{2+} waves, whereas cells obtained from a healthy 32-year-old female without history of cardiac disease served as control. In accordance with the CPVT phenotype, where patients show a normal ECG pattern under baseline conditions, only few untreated cells displayed Ca^{2+} waves (Figure 6), whereas beta-adrenergic stimulation induced by ISO led to a significant increase in diastolic Ca^{2+} waves in $RyR2^{S406L/WT}$ cells but did not induce Ca^{2+} waves in control cells. Treatment of $RyR2^{S406L}$ cells with either efsevin or kaempferol significantly reduced the number of cells displaying Ca^{2+} waves and the average frequency of Ca^{2+} waves per minute to baseline levels.

FIGURE 4 Efsevin Reduces Intracellular Ca^{2+} Spark Frequency, Amplitude, and Cytosolic Ca^{2+} Clearance Leading to a Restriction of Individual Ca^{2+} Sparks

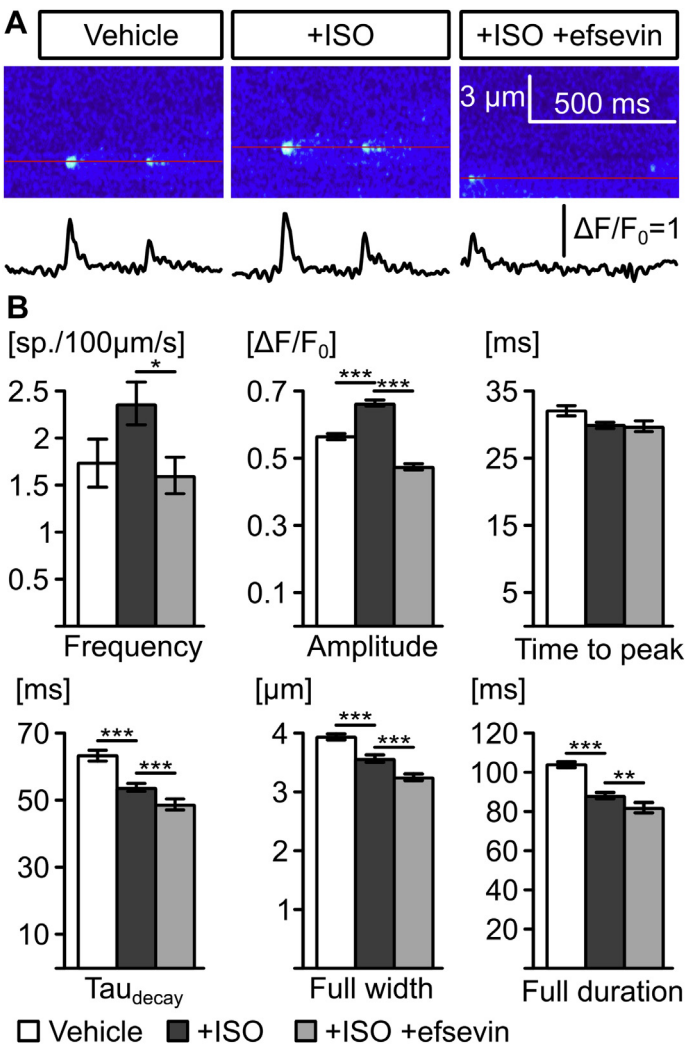

(A) Representative line scan confocal images from $RyR2^{R4496C/WT}$ cardiomyocytes show spontaneous Ca^{2+} sparks. **(B)** Treatment with ISO induced a higher spark frequency and amplitude and accelerated cytosolic Ca^{2+} removal (tau_{decay}) leading to narrower (full width) and shorter (full duration) sparks. Administration of efsevin reduced Ca^{2+} spark frequency ($p = 0.049$, Kruskal Wallis test) and amplitude ($p < 0.001$, Kruskal Wallis test) and limited spatial ($p < 0.001$, Kruskal Wallis test) and temporal ($p = 0.002$, Kruskal Wallis test) expansion of Ca^{2+} sparks. *$p < 0.05$; **$p < 0.01$; ***$p < 0.001$. Abbreviations as in Figure 1.

DISCUSSION

MITOCHONDRIA AS DRUG TARGETS. Mitochondria occupy approximately 30% of the cardiomyocyte volume (6,7). Although their crucial roles in ATP synthesis, regulation of respiratory rate, and apoptosis are well understood, mitochondrial contributions to cardiac Ca^{2+} handling are still under debate. While it is generally accepted that a gradual and moderate rise in mitochondrial Ca^{2+} enhances energy production (18), the role of a low-affinity/high-conductance, fast mitochondrial Ca^{2+} uptake remains unclear. Different experimental approaches suggest an immediate role for this uptake in the regulation of cardiomyocyte bioenergetics (38), contraction (39), and rhythmicity (15,21), but the potential of this rapid mitochondrial Ca^{2+} uptake mechanism to serve as a drug target in cardiovascular disease has not been sufficiently evaluated. It was proposed that inhibition of MCU by Ru360 ameliorates myocardial damage after ischemia reperfusion injury in rats, presumably by inhibiting depolarization of mitochondria and following opening of the mitochondrial permeability transition pore (40).

FIGURE 5 MiCUps Reduce Episodes of Ventricular Tachycardia in $RyR2^{R4496C/WT}$ Mice

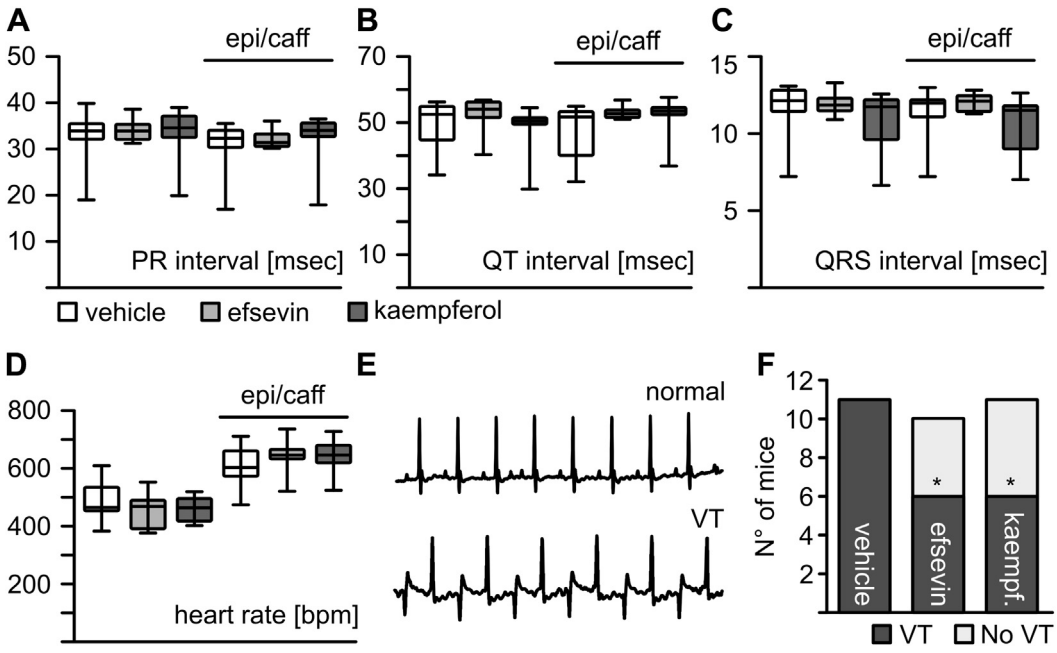

Three-lead surface ECGs from $RyR2^{R4496C/WT}$ mice receiving efsevin or kaempferol through an osmotic minipump are shown. After a baseline ECG was recorded, mice were injected with epi/caff as an adrenergic stimulus. Basic parameters of the ECG like PR **(A)**, QT **(B)**, and QRS **(C)** intervals were comparable between the vehicle-treated group and both of the MiCUp-treated groups at baseline and after epi/caff challenge (Kruskal-Wallis test). **(D)** Heart rate increased upon administration of epi/caff in all 3 groups but remained unaffected by the administration of MiCUps (Kruskal-Wallis test). **(E)** Examples of a normal ECG recording and a recording showing bidirectional ventricular tachycardia. **(F)** Episodes of bidirectional ventricular tachycardia were recorded in 11 of 11 vehicle-treated mice but were significantly reduced to 6 of 10 in mice with efsevin and 6 of 11 in mice with kaempferol ($p = 0.035$, Fisher's exact test). *$p < 0.05$. ECG = electrocardiography; epi/caff = epinephrine/caffeine; MiCUp = mitochondrial calcium uptake enhancer.

However, in healthy myocardium, the role of fast mitochondrial Ca^{2+} uptake remains elusive. Regarding arrhythmia, protective (22) as well as pro-arrhythmic (41) effects of activated mitochondria were discussed. We have recently identified the novel compound efsevin, which binds to the outer mitochondrial membrane VDAC2, enhances mitochondrial Ca^{2+} uptake, and restores rhythmic cardiac contractions in a zebrafish model for Ca^{2+}-induced cardiac arrhythmia (15). Here we show that enhancing mitochondrial Ca^{2+} uptake by using MiCUps efficiently suppresses arrhythmia in a murine and a human model of CPVT in vitro and in vivo. Our results establish pharmacological activation of rapid mitochondrial Ca^{2+} uptake as a novel preventive and therapeutic strategy against CPVT. We have previously shown that efsevin suppresses arrhythmia in cellular models for Ca^{2+} overload induced by high extracellular Ca^{2+} (15). Thus, due to their potent role of suppressing arrhythmogenic Ca^{2+} waves in both Ca^{2+} overload (15) and CPVT, it is conceivable that MiCUps may also be applied in other more common forms of Ca^{2+}-induced cardiac arrhythmias. These include arrhythmias in the setting of heart failure, which are triggered by cellular Ca^{2+} overload or atrial fibrillation, also linked to imbalances in cardiomyocyte Ca^{2+} handling (5). This study serves as a proof-of-principle, holding great promise for additional indications.

OPTIMIZED MiCUps. Our work shows that enhancing mitochondrial Ca^{2+} uptake efficiently reduces arrhythmia in experimental models of CPVT. In order to develop MiCUps toward human therapeutics, several steps of optimization must be taken. Candidate compounds need to be optimized to achieve a high affinity MiCUp with low side effects and suitable pharmacokinetics for application in human subjects. We show that the antiarrhythmic effect can be achieved by activation of at least 2 distinct target proteins within the mitochondrial Ca^{2+} uptake complex: efsevin, targeting VDAC2 in the outer mitochondrial membrane, and kaempferol, targeting MCU in the

FIGURE 6 **MiCUps Reduce Spontaneous Ca^{2+} Waves in Human iPSC-derived Cardiomyocytes**

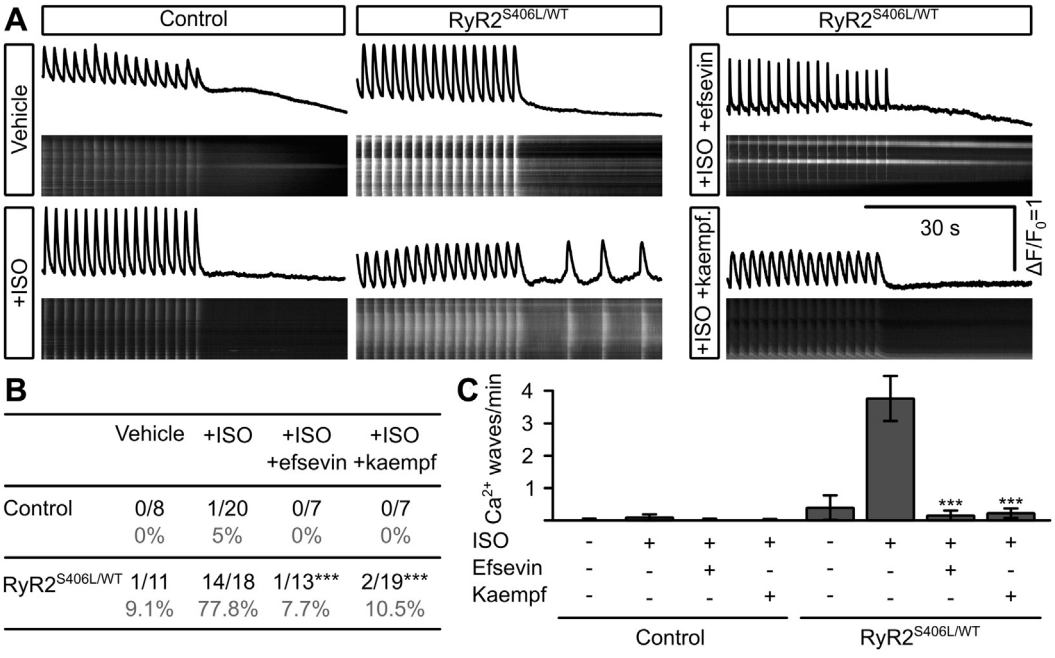

Confocal line scans of iPSC-derived human cardiomyocytes from a CPVT patient ($RyR2^{S406L/WT}$) and a healthy individual are shown (control). **(A)** Confocal line scans across iPSC-derived human cardiomyocytes loaded with Fluo-4 AM to measure intracellular Ca^{2+} and intensity plots show that stimulation with ISO does not induce spontaneous, diastolic Ca^{2+} waves in control cells but induced waves in $RyR2^{S406L/WT}$ cardiomyocytes. These waves can be blocked with either 15 μM efsevin **(upper right panel)** or 10 μM kaempferol **(lower right panel)**. **(B)** Quantitative analysis revealed a significant reduction in the number of $RyR2^{S406L/WT}$ cells showing ISO-induced Ca^{2+} waves upon treatment with MiCUps, to a level comparable to that of unstimulated cells (**asterisks** denote significance compared to $RyR2^{S406L/WT}$ +ISO by Fisher's exact test). **(C)** Quantification of waves/min reveal a significant reduction from 3.78 ± 0.72 waves/min in $RyR2^{S406L/WT}$ cardiomyocytes treated with ISO to levels indistinguishable from control after treatment with efsevin (0.15 ± 0.15; $p < 0.001$ compared to ISO: $p = 0.884$ compared to vehicle, Kruskal-Wallis test) or kaempferol, respectively (0.21 ± 0.14, $p < 0.001$ compared to ISO; $p = 0.980$ compared to vehicle, Kruskal-Wallis test). ***$p < 0.001$. CPVT = catecholaminergic polymorphic ventricular tachycardia; iPSC = induced pluripotent stem cell; other abbreviations as in Figure 1.

inner membrane. Suppression of arrhythmia is thus attributable to enhanced mitochondrial Ca^{2+} uptake and is independent of the molecular target protein within the fast mitochondrial Ca^{2+} uptake complex. Our work thus establishes the entire protein complex as a pharmacological target structure and allows for future optimization of this therapeutic concept through novel compounds and targets. Apart from VDAC2 and MCU, the auxiliary MCU regulators MICU1 and -2, MCUb, EMRE, and MCUR1 (16,17) may serve as future candidate targets.

SIDE EFFECTS. Mitochondrial Ca^{2+} uptake proteins such as VDAC2 and MCU are ubiquitously expressed. Regarding a therapeutic application, it is thus important to evaluate potential side effects of a MiCUp-based therapy. It is important to note that we did not observe any adverse effects of MiCUps in mice treated with efsevin or kaempferol for 3 to 8 consecutive days. Furthermore, kaempferol was previously used in animal experiments, and no adverse effects, even after up to 1 year of treatment or at high doses, were observed (42-44). However, further long-term experiments and large animal studies are needed to further evaluate safety of a MiCUp-based therapy. Although we did not observe changes in cytosolic Ca^{2+} in our experiments, long-term effects of enhanced mitochondrial Ca^{2+} uptake on a potential redistribution of cellular Ca^{2+} in the heart and other organs must be evaluated. Furthermore, because an enhanced mitochondrial Ca^{2+} uptake was observed to activate mitochondrial metabolism and reactive oxygen species production, special focus should be directed toward side effects related to changes in cellular bioenergetics.

Common side effects of actual antiarrhythmic drugs like Na^{+}, K^{+}, and Ca^{2+} channel blockers include

changes in cardiac electrophysiology like deceleration of cardiac de- or repolarization, the latter often expressed as a prolonged QT interval. We observed an effect of efsevin on the repolarization phase of the action potential in mice (Supplemental Figure 1), namely a prolongation of APD50 but not APD90. However, whereas repolarization in mice is carried mainly by fast potassium currents ($I_{to,}$ $I_{K,\ slow}$), the human action potential displays a pronounced plateau phase, and phase 3 repolarization is carried predominantly by the delayed K^+ currents I_{Kr} and I_{ks} (32). To rule out the possibility that the observed prolongation of APD50 by efsevin in mice could be relevant for human therapy, we showed that efsevin does not influence action potential duration in human iPSC-derived cardiomyocytes and does not block hERG activity. It is thus conceivable that efsevin has a direct impact on the fast repolarizing currents in mice but does not influence the human action potential. Most importantly, however, we did not observe effects of MiCUp administration on ECG parameters like PR, QT, and QRS interval and heart rate in mice treated with MiCUps. Because MiCUps target intracellular structures to suppress the generation of ectopic depolarizations and do not influence the cardiac action potential, they might be less prone to severe side effects like, for example, the typical pro-arrhythmic effects observed with class I or III antiarrhythmic drugs. However, the murine repertoire of ion channels governing the cardiac action potential of mice varies from the human one, and additional experiments in other mammalian species are needed to solve this issue.

CONCLUSIONS

Common antiarrhythmic drugs aim at inhibiting expansion of ectopic activity and display perilous side effects. Because major arrhythmias are often associated with imbalanced intracellular Ca^{2+} homeostasis (3–5), intracellular Ca^{2+} transporters are attractive candidates for newer and safer therapies. Here we show that enhancing mitochondrial Ca^{2+} uptake by pharmacological agonists of the mitochondrial Ca^{2+} uptake proteins VDAC2 and MCU efficiently suppresses arrhythmia in a murine and a human model for CPVT. Our data establish MiCUps as attractive compounds for a novel preventive and therapeutic strategy to treat Ca^{2+}-triggered cardiac arrhythmias.

ACKNOWLEDGEMENTS The authors thank Brigitte Mayerhofer for technical assistance and Petra Eigner, Monika Mittermeier, and Clarinda Hofer and the staff of the Institute for Biomedical Research of the Medical University of Graz for animal husbandry.

ADDRESS FOR CORRESPONDENCE: Dr. Johann Schredelseker, Walther Straub Institute of Pharmacology and Toxicology, Ludwig-Maximilians-Universität München Nußbaumstrasse 26, D-80336 München, Germany. E-mail: johann.schredelseker@lmu.de.

PERSPECTIVES

COMPETENCY IN MEDICAL KNOWLEDGE: Mitochondria regulate cardiac rhythmicity. Pharmacological activation of mitochondrial Ca^{2+} uptake by MiCUps suppresses arrhythmogenesis in murine and human iPSC-based models for catecholaminergic polymorphic ventricular tachycardia.

TRANSLATIONAL OUTLOOK 1: Optimization of compounds and a careful investigation on pharmacokinetics and drug metabolism are needed to develop a potential MiCUp-based human therapy.

TRANSLATIONAL OUTLOOK 2: Additional experiments using models of other Ca^{2+}-triggered arrhythmias could further expand the application range of MiCUps.

REFERENCES

1. Mozaffarian D, Benjamin EJ, Go AS, et al. Heart disease and stroke statistics-2016 update. Circulation 2016;133:e38–360.

2. Mehra R. Global public health problem of sudden cardiac death. J Electrocardiol 2007;40:S118–22.

3. Bers DM. Calcium and cardiac rhythms: physiological and pathophysiological. Circ Res 2002;90:14–7.

4. Choi B-R, Burton F, Salama G. Cytosolic Ca^{2+} triggers early afterdepolarizations and Torsade de Pointes in rabbit hearts with type 2 long QT syndrome. J Physiol 2002;543:615–31.

5. Greiser M, Lederer WJ, Schotten U. Alterations of atrial Ca^{2+} handling as cause and consequence of atrial fibrillation. Cardiovasc Res 2011;89:722–33.

6. Barth E, Stämmler G, Speiser B, Schaper J. Ultrastructural quantitation of mitochondria and myofilaments in cardiac muscle from 10 different animal species including man. J Mol Cell Cardiol 1992;24:669–81.

7. Kim H-D, Kim CH, Rah Bb-J, Chung H-I, Shim T-S. Quantitative study on the relation between structural and functional properties of the hearts from three different mammals. Anat Rec 1994;238:199–206.

8. Szalai G, Csordás G, Hantash BM, Thomas AP, Hajnóczky G. Calcium signal transmission between ryanodine receptors and mitochondria. J Biol Chem 2000;275:15305–13.

9. Dorn GW, Maack C. SR and mitochondria: calcium cross-talk between kissing cousins. J Mol Cell Cardiol 2013;55:42–9.

10. Kirichok Y, Krapivinsky G, Clapham DE. The mitochondrial calcium uniporter is a highly selective ion channel. Nature 2004;427:360–4.

11. Baughman JM, Perocchi F, Girgis HS, et al. Integrative genomics identifies MCU

as an essential component of the mitochondrial calcium uniporter. Nature 2011;476:341–5.

12. De Stefani D, Raffaello A, Teardo E, Szabò I, Rizzuto R. A forty-kilodalton protein of the inner membrane is the mitochondrial calcium uniporter. Nature 2011;476:336–40.

13. Subedi KP, Kim J-C, Kang M, Son M-J, Kim Y-S, Woo S-H. Voltage-dependent anion channel 2 modulates resting Ca^{2+} sparks, but not action potential-induced Ca^{2+} signaling in cardiac myocytes. Cell Calcium 2011;49:136–43.

14. Min CK, Yeom DR, Lee K-E, et al. Coupling of ryanodine receptor 2 and voltage-dependent anion channel 2 is essential for Ca^{2+} transfer from the sarcoplasmic reticulum to the mitochondria in the heart. Biochem J 2012;447:371–9.

15. Shimizu H, Schredelseker J, Huang J, et al. Mitochondrial Ca^{2+} uptake by the voltage-dependent anion channel 2 regulates cardiac rhythmicity. Elife 2015;4.

16. Jhun BS, Mishra J, Monaco S, et al. The mitochondrial Ca^{2+} uniporter: regulation by auxiliary subunits and signal transduction pathways. Am J Physiol Cell Physiol 2016;311:C67–80.

17. Marchi S, Pinton P. The mitochondrial calcium uniporter complex: molecular components, structure and physiopathological implications. J Physiol 2014;592:829–39.

18. Brandes R, Bers DM. Intracellular Ca^{2+} increases the mitochondrial NADH concentration during elevated work in intact cardiac muscle. Circ Res 1997;80:82–7.

19. Williams GSB, Boyman L, Chikando AC, Khairallah RJ, Lederer WJ. Mitochondrial calcium uptake. Proc Natl Acad Sci U S A 2013;110:10479–86.

20. O'Rourke B, Blatter LA. Mitochondrial Ca^{2+} uptake: tortoise or hare? J Mol Cell Cardiol 2009;46:767–74.

21. Seguchi H, Ritter M, Shizukuishi M, et al. Propagation of Ca^{2+} release in cardiac myocytes: role of mitochondria. Cell Calcium 2005;38:1–9.

22. Zhao Z, Gordan R, Wen H, Fefelova N, Zang W-J, Xie L-H. Modulation of intracellular calcium waves and triggered activities by mitochondrial ca flux in mouse cardiomyocytes. PLoS One 2013;8:e80574.

23. Priori SG, Napolitano C, Tiso N, et al. Mutations in the cardiac ryanodine receptor gene (hRyR2) underlie catecholaminergic polymorphic ventricular tachycardia. Circulation 2001;103:196–200.

24. Cerrone M, Colombi B, Santoro M, et al. Bidirectional ventricular tachycardia and fibrillation elicited in a knock-in mouse model carrier of a mutation in the cardiac ryanodine receptor. Circ Res 2005;96:e77–82.

25. O'Connell TD, Rodrigo MC, Simpson PC. Isolation and culture of adult mouse cardiac myocytes. Methods Mol Biol 2007;357:271–96.

26. Jung CB, Moretti A, Mederos y Schnitzler M, et al. Dantrolene rescues arrhythmogenic RYR2 defect in a patient-specific stem cell model of catecholaminergic polymorphic ventricular tachycardia. EMBO Mol Med 2012;4:180–91.

27. Moretti A, Bellin M, Welling A, et al. Patient-specific induced pluripotent stem-cell models for long-QT syndrome. N Engl J Med 2010;363:1397–409.

28. Claycomb WC, Lanson NA, Stallworth BS, et al. HL-1 cells: a cardiac muscle cell line that contracts and retains phenotypic characteristics of the adult cardiomyocyte. Proc Natl Acad Sci U S A 1998;95:2979–84.

29. Sharma VK, Ramesh V, Franzini-Armstrong C, Sheu SS. Transport of Ca^{2+} from sarcoplasmic reticulum to mitochondria in rat ventricular myocytes. J Bioenerg Biomembr 2000;32:97–104.

30. Paavola J, Viitasalo M, Laitinen-Forsblom PJ, et al. Mutant ryanodine receptors in catecholaminergic polymorphic ventricular tachycardia generate delayed afterdepolarizations due to increased propensity to Ca^{2+} waves. Eur Heart J 2007;28:1135–42.

31. Allen DG, Eisner DA, Orchard CH. Characterization of oscillations of intracellular calcium concentration in ferret ventricular muscle. J Physiol 1984;352:113–28.

32. Nerbonne JM, Nichols CG, Schwarz TL, Escande D. Genetic manipulation of cardiac K^+ channel function in mice: what have we learned, and where do we go from here? Circ Res 2001;89:944–56.

33. Montero M, Lobatón CD, Hernández-Sanmiguel E, et al. Direct activation of the mitochondrial calcium uniporter by natural plant flavonoids. Biochem J 2004;384:19–24.

34. Vay L, Hernández-Sanmiguel E, Santo-Domingo J, et al. Modulation of Ca^{2+} release and Ca^{2+} oscillations in HeLa cells and fibroblasts by mitochondrial Ca^{2+} uniporter stimulation. J Physiol 2007;580:39–49.

35. Jiang D, Xiao B, Zhang L, Chen SRW. Enhanced basal activity of a cardiac Ca^{2+} release channel (ryanodine receptor) mutant associated with ventricular tachycardia and sudden death. Circ Res 2002;91:218–25.

36. Fernández-Velasco M, Rueda A, Rizzi N, et al. Increased Ca^{2+} sensitivity of the ryanodine receptor mutant $RyR2^{R4496C}$ underlies catecholaminergic polymorphic ventricular tachycardia. Circ Res 2009;104:201–9.

37. Sedej S, Heinzel FR, Walther S, et al. Na^+-dependent SR Ca^{2+} overload induces arrhythmogenic events in mouse cardiomyocytes with a human CPVT mutation. Cardiovasc Res 2010;87:50–9.

38. Tomar D, Dong Z, Shanmughapriya S, et al. MCUR1 Is a scaffold factor for the MCU complex function and promotes mitochondrial bioenergetics. Cell Rep 2016;15:1673–85.

39. Drago I, De Stefani D, Rizzuto R, Pozzan T. Mitochondrial Ca^{2+} uptake contributes to buffering cytoplasmic Ca^{2+} peaks in cardiomyocytes. Proc Natl Acad Sci U S A 2012;109:12986–91.

40. García-Rivas G, de J, Carvajal K, Correa F, Zazueta C. Ru360, a specific mitochondrial calcium uptake inhibitor, improves cardiac post-ischaemic functional recovery in rats in vivo. Br J Pharmacol 2006;149:829–37.

41. Xie W, Santulli G, Reiken SR, et al. Mitochondrial oxidative stress promotes atrial fibrillation. Sci Rep 2015;5:11427.

42. Song H, Bao J, Wei Y, et al. Kaempferol inhibits gastric cancer tumor growth: An in vitro and in vivo study. Oncol Rep 2014;33:868–74.

43. Montero M, de la Fuente S, Fonteriz RI, Moreno A, Alvarez J. Effects of long-term feeding of the polyphenols resveratrol and kaempferol in obese mice. PLoS One 2014;9:e112825.

44. Shih T-Y, Young T-H, Lee H-S, Hsieh C-B, Hu OY-P. Protective effects of kaempferol on isoniazid- and rifampicin-induced hepatotoxicity. AAPS J 2013;15:753–62.

KEY WORDS CPVT, MCU, MiCUp, mitochondria, RyR2, VDAC2

APPENDIX For expanded Methods section as well as supplemental figures, please see the online version of this article.

9 Paper 2: The antiarrhythmic compound efsevin directly modulates voltage-dependent anion channel 2 by binding to its inner wall and enhancing mitochondrial Ca^{2+} uptake

Received: 12 April 2019 | Revised: 20 January 2020 | Accepted: 29 January 2020

DOI: 10.1111/bph.15022

RESEARCH PAPER

The antiarrhythmic compound efsevin directly modulates voltage-dependent anion channel 2 by binding to its inner wall and enhancing mitochondrial Ca^{2+} uptake

Fabiola Wilting[1] | Robin Kopp[1] | Philip A. Gurnev[2] | Anna Schedel[1] | Nathan J. Dupper[3] | Ohyun Kwon[3] | Annette Nicke[1] | Thomas Gudermann[1,4] | Johann Schredelseker[1]

[1]Walther Straub Institute of Pharmacology and Toxicology, Faculty of Medicine, LMU Munich, Munich, Germany

[2]Section on Molecular Transport, Eunice Kennedy Shriver National Institute of Child Health and Human Development, National Institutes of Health, Bethesda, Maryland

[3]Department of Chemistry and Biochemistry, University of California Los Angeles, Los Angeles, California

[4]Deutsches Zentrum für Herz-Kreislauf-Forschung (DZHK), Partner Site Munich Heart Alliance (MHA), Munich, Germany

Correspondence
Johann Schredelseker, Walther Straub Institute of Pharmacology and Toxicology, LMU Munich, Munich 80336, Germany.
Email: johann.schredelseker@lmu.de

Funding information
Deutsche Forschungsgemeinschaft, Grant/Award Number: SCHR 1471/1-1; U.S. National Institute of Health, Grant/Award Number: R01GM071779

Background and Purpose: The synthetic compound efsevin was recently identified to suppress arrhythmogenesis in models of cardiac arrhythmia, making it a promising candidate for antiarrhythmic therapy. Its activity was shown to be dependent on the voltage-dependent anion channel 2 (VDAC2) in the outer mitochondrial membrane. Here, we investigated the molecular mechanism of the efsevin–VDAC2 interaction.

Experimental Approach: To evaluate the functional interaction of efsevin and VDAC2, we measured currents through recombinant VDAC2 in planar lipid bilayers. Using molecular ligand-protein docking and mutational analysis, we identified the efsevin binding site on VDAC2. Finally, physiological consequences of the efsevin-induced modulation of VDAC2 were analysed in HL-1 cardiomyocytes.

Key Results: In lipid bilayers, efsevin reduced VDAC2 conductance and shifted the channel's open probability towards less anion-selective closed states. Efsevin binds to a binding pocket formed by the inner channel wall and the pore-lining N-terminal α-helix. Exchange of amino acids N207, K236 and N238 within this pocket for alanines abolished the channel's efsevin-responsiveness. Upon heterologous expression in HL-1 cardiomyocytes, both channels, wild-type VDAC2 and the efsevin-insensitive $VDAC2^{AAA}$ restored mitochondrial Ca^{2+} uptake, but only wild-type VDAC2 was sensitive to efsevin.

Conclusion and Implications: In summary, our data indicate a direct interaction of efsevin with VDAC2 inside the channel pore that leads to modified gating and results in enhanced SR-mitochondria Ca^{2+} transfer. This study sheds new light on the function of VDAC2 and provides a basis for structure-aided chemical optimization of efsevin.

Abbreviations: CPVT, catecholaminergic polymorphic ventricular tachycardia; DPhPC, 1,2-diphytanoyl-sn-glycero-3-phosphatidylcholine; hVDAC2, human voltage-dependent anion channel 2; IRES, internal ribosome entry site; MCU, mitochondrial calcium uniporter; MOI, multiplicity of infection; mVDAC2, mouse voltage-dependent anion channel 2; OMM, outer mitochondrial membrane; P_O, open probability; RuR, ruthenium red; shRNA, short hairpin RNA; SR, sarcoplasmic reticulum; VDAC, voltage-dependent anion channel; zVDAC2, zebrafish voltage-dependent anion channel 2.

1 | INTRODUCTION

Cardiovascular diseases represent the primary cause of death and hospitalization worldwide (Benjamin et al., 2018). Especially, Cardiac arrhythmias are difficult to treat due to major side effects of common antiarrhythmic drugs. It is thus a major focus of cardiovascular research to identify novel, safer therapies for cardiac arrhythmia.

Using a chemical suppressor screen on the zebrafish cardiac arrhythmia model *tremblor* (Ebert et al., 2005; Langenbacher et al., 2005), we have previously identified the synthetic compound efsevin, a dihydropyrrole carboxylic ester compound, which potently restored rhythmic cardiac contractions in otherwise fibrillating zebrafish embryonic hearts (Shimizu et al., 2015). We further demonstrated efficacy of efsevin in translational models for catecholaminergic polymorphic ventricular tachycardia (CPVT; Schweitzer et al., 2017). Here, efsevin reduced episodes of tachycardia in vivo in CPVT mice and suppressed arrhythmogenic events in induced pluripotent stem cell-derived cardiomyocytes from a CPVT patient (Schweitzer et al., 2017). These findings make efsevin a promising lead structure for human antiarrhythmic therapy.

In a pull-down assay with immobilized efsevin, the outer mitochondrial membrane (OMM) voltage-dependent anion channel 2 (VDAC2) was identified as the primary molecular target of efsevin (Shimizu et al., 2015). Voltage-dependent anion channels are large pore-forming proteins in the outer mitochondrial membrane. They represent the main pathway for ions and metabolites over the outer mitochondrial membrane. Three isoforms of voltage-dependent anion channels are expressed in vertebrates out of which VDAC2 was described to have a specific role in the heart. While a global knockout of VDAC2 in mice is embryonically lethal (Cheng, Sheiko, Fisher, Craigen, & Korsmeyer, 2003), a conditional heart-specific VDAC2 knockout mouse was reported to develop post-natal cardiac defects and to die shortly after birth (Raghavan, Sheiko, Graham, & Craigen, 2012). In cardiomyocytes, VDAC2 was described to interact with the **ryanodine receptor** (RyR; Min et al., 2012) and to modulate cytosolic Ca^{2+} signals (Shimizu et al., 2015; Subedi et al., 2011). In arrhythmic *tremblor* zebrafish embryos, efsevin induced a restoration of rhythmic cardiac contractions. Transient knock-down of VDAC2 abolished the efsevin induced phenotype restoration while overexpression of VDAC2 recovered it. In cultured cells, efsevin enhanced uptake of Ca^{2+} into mitochondria. A direct link between the enhanced mitochondrial Ca^{2+} uptake and efsevin's anti-arrhythmic properties was established by two lines of experiments: (a) Pharmacological inactivation of mitochondrial Ca^{2+} uptake by Ru360, an inhibitor of the mitochondrial Ca^{2+} uniporter (MCU), abolished efsevin's protective effect in CPVT cardiomyocytes and (b) kaempferol, an activator of the mitochondrial Ca^{2+} uniporter, reduced arrhythmogenic Ca^{2+} signals comparable to efsevin (Schweitzer et al., 2017).

However, biophysical and structural determinants of the efsevin–VDAC2 interaction have remained unexplored. It is still unclear whether efsevin directly interacts with the VDAC2 peptide and thereby modulates the electrophysiological properties of the channel or if the observed effects require a yet unidentified protein partner. To address this issue, we expressed and purified recombinant zebrafish VDAC2 (zVDAC2) protein and inserted it into planar lipid bilayers. We found a pronounced effect of efsevin on channel gating and opening probability, indicating a direct effect of efsevin on the channel. To analyse the structural basis of the efsevin VDAC2 interaction, we performed computational protein-ligand docking using the crystal structure of zVDAC2 (Schredelseker et al., 2014). VDAC2 is formed by a barrel-like structure consisting of 19 antiparallel β-sheets (β-sheets 1-19) and an N-terminal α-helix lining the inner channel wall (Schredelseker et al., 2014). We identified an efsevin binding site located in a groove between the inner channel wall and the pore-lining α-helix and formed by hydrogen bonds and hydrophobic interactions between efsevin and the zVDAC2 peptide. Replacement of three residues (N207, K236 and N238) from this binding site with alanines ($zVDAC2^{AAA}$) resulted in a complete loss of efsevin sensitivity. To evaluate the physiological consequence of the observed efsevin-induced biophysical changes in VDAC2, we heterologously expressed wild-type zVDAC2 and the efsevin-insensitive $zVDAC2^{AAA}$ mutant in cultured HL-1 cardiomyocytes. We demonstrate that the observed changes in zVDAC2 electrophysiology translate into enhanced mitochondrial Ca^{2+} uptake and thereby explain the antiarrhythmic effect of efsevin. Our data provide novel insights into VDAC2 function and provide a basis for structure-aided chemical optimization of efsevin as a lead structure for the development of novel antiarrhythmic drugs.

What is already known

- The synthetic compound efsevin suppresses arrhythmogenesis in cardiac arrhythmia models.
- Efsevin binds to the mitochondrial voltage-dependent anion channel anion channel 2 (VDAC2).

What this study adds

- Efsevin binds into a pocket formed by the channel wall and the pore-lining helix.
- Efsevin facilitates VDAC2 gating into a less anion-selective state and enhances Ca^{2+} flux.

What is the clinical significance

- Identification of mode of action and binding pocket allows for future structure aided-drug optimization.

2 | METHODS

2.1 | Expression and purification of zVDAC2

Expression and purification of zVDAC2 were performed as previously described (Schredelseker et al., 2014) with minor modifications: Histidine-tagged zVDAC2 was purified on an Äkta pure chromatography system using a HisPrep FF 16/10 column. After refolding dialysis, size exclusion chromatography was performed on a HiLoad 16/600 Superdex200 pg column equilibrated with 150-mM NaCl, 1-mM DTT, 0.1% LDAO, and 20-mm Tris-HCl (pH = 8.0). Integrity of the purified zVDAC2 was confirmed by SDS-PAGE analysis on a 12% gel.

2.2 | Planar lipid bilayer recordings

Painted planar lipid bilayers were formed on an Ionovation Bilayer Explorer lipid bilayer set-up across a 120-μm diameter opening with 1,2-diphytanoyl-sn-glycero-3-phosphatidylcholine (DPhPC) dissolved in *n*-decane at 12.5 mg·ml^{-1}. Both chambers were filled with 1-M KCl, 5-mM $CaCl_2$, and 10-mM Tris-HCl (pH = 7.2) To facilitate insertion, purified zVDAC2 was inserted into lipidic bicelles (Ujwal, 2012). After formation of a stable bilayer, zVDAC2 containing bicelles were added to the cis chamber. After insertion of a channel, the membrane was clamped to 0 mV, and 10 s pulses to test potentials from −60 mV to +60 mV were applied. The signal was sampled at 10 kHz and filtered at 2 kHz. Efsevin (50-μM stock in recording solution) was added to the cis chamber to a final concentration of 8 μM. Data analysis was performed using Nest-o-Patch (Dr. V. Nesterov, https://sourceforge.netq/projects/nestopatch/).

zVDAC2 ion selectivity was measured using folded planar membranes formed from opposition of two monolayers made of 5 mg·ml^{-1} solution of DPhPC in pentane, as described (Rostovtseva, Gurnev, Chen, & Bezrukov, 2012). Recordings were performed in the buffer described above. Channel insertion was achieved by adding zVDAC2 in a 2.5% Triton X-100 solution to the cis compartment while stirring. After single channel was inserted in symmetrical solutions, the cis side was perfused with Tris-HCl (pH 7.2) buffer solution to achieve 0.2-M KCl. The exact KCl concentration of 0.2 M in the cis compartment after perfusion was verified at the end of each selectivity experiment using a conductivity meter CDM230 (Radiometer analytical). Ion selectivity of zVDAC2 conductance states was calculated from the reversal potential (V_{rev}). Permeability ratio between Cl^-, and K^+, I^-/I^+, was calculated according to the Goldman–Hodgkin–Katz equation (Hille, 2001):

$$I^-/I^+ = \left(1 - \frac{V_{rev}}{\frac{k_B T}{e} \cdot ln\frac{a_{trans}}{a_{cis}}}\right) \cdot \left(1 + \frac{V_{rev}}{\frac{k_B T}{e} \cdot ln\frac{a_{trans}}{a_{cis}}}\right)^{-1},$$

where k_B, T, and e have their usual meaning of Boltzmann constant, absolute temperature, and electron charge, and KCl solution activities were a_{cis} = 0.144 for 0.2-M KCl and a_{trans} = 0.604 for 1-M KCl, respectively (Lide, 2006).

2.3 | Molecular docking

The three-dimensional (3D) structure of efsevin was generated using MarvinSketch (v15.1.9, ChemAxon) and saved in the .pdb format. The crystal structure of zVDAC2 was obtained from the Research Collaboratory for Structural Bioinformatics Protein Data Bank (PDB ID: 4BUM). Gasteiger charges and hydrogens were added to protein and ligand using AutoDockTools (v1.5.6; Morris et al., 2009), and AutoDock Vina was used to perform the molecular docking simulations (Trott & Olson, 2010). The term "independent docking experiment" used in this text refers to independent software runs of AutoDock Vina. Each run starts from a random conformation that is independent from the previous one and yields nine likely conformations. To determine the best hypothetical binding mode of efsevin on zVDAC2, the flexible form of efsevin was first docked to the rigid zVDAC2 structure. After 15 iterative dockings with a grid centred to ensure coverage of the entire channel, analysis of 135 binding conformations showed that the binding site with the lowest binding energy was found in the region between the inner channel wall and the highly flexible N-terminal α-helix. Since zVDAC2 might undergo conformational changes upon binding of efsevin, the side chains facing the potential binding site were kept flexible for subsequent dockings (N19, Y22, F24, N207, R218, K236, N238, L242 and L262). The grid box was narrowed to 24 Å × 20 Å × 20 Å to cover this region. After additional 15 iterative dockings with flexible side chains, the best binding poses were selected based on the predicted binding affinities. Interactions were analysed with LigPlot+ (Laskowski & Swindells, 2011).

2.4 | Molecular cloning

To introduce N207A, K236A and N238A into pQE60-zVDAC2 for recombinant expression and purification construct pQE60-zVDAC2^{AAA} was created by two mutagenesis PCR reactions using pQE60-zVDAC2 (Schredelseker et al., 2014) as a template. The two PCR fragments were fused by overlap extension PCR and the resulting product was ligated into pQE60-zVDAC2 with PstI and NheI.

For the creation of pCClc-CMV-zVDAC2-IRES-nlsEGFP for virus production and following transduction of zVDAC2 into HL-1 cells, eGFP with a nuclear localization signal (nls-eGFP) together with an internal ribosome entry site (IRES) was PCR-amplified from p3E-IRES-nlsEGFPpA (Kwan et al., 2007) and subcloned into pCS2+ containing the zVDAC2 open reading frame (Shimizu et al., 2015). The zVDAC2-IRES-nlsEGFP construct was fused into pCCLc-CMV using the In-Fusion HD Cloning Kit (TaKaRa).

For the creation of pCClc-CMV-zVDAC2^{AAA}-IRES-nlsEGFP, zVDAC2 was exchanged for zVDAC2^{AAA} in pCS2+-zVDAC2 (Shimizu

et al., 2015) by PCR amplification of the zVDAC2^{AAA} open reading frame from PQE60-zVDAC2^{AAA} following ligation with BamHI and ClaI. The open reading frame of zVDAC2^{AAA} was PCR-amplified from pCS2+-zVDAC2^{AAA} fused to the IRES PCR-amplified from pCClc-CMV-zVDAC2-IRES-nlsEGFP by SOE PCR and the resulting fragment was fused into pCClc-CMV-zVDAC2-IRES-nlsGFP using the In-Fusion HD Cloning Kit (TaKaRa).

2.5 | Production of lentiviruses

Recombinant lentiviruses were produced in HEK 293T cells. Briefly, cells at 40% confluency were cotransfected with pCCLc-CMV-zVDAC2-IRES-nlsEGFP or pCCLc-CMV-zVDAC2^{AAA}-IRES-nlsEGFP together with pCMVΔ8.91 (coding for gag, pol, rev) and pCAGGS-VSV-G at a 5:5:1 ratio using TransIT®-293 (Mirus). Cells were induced with 10-mM sodium butyrate on the following day. The supernatant containing the virus was collected on Day 3 after transfection, filtered through a 0.45-μm syringe filter, and stored at −80°C. Viral titres were determined using the Lenti-X™ qRT-PCR Titration Kit (Takara).

2.6 | HL-1 culture and creation of cell lines

HL-1 cells were cultured as described previously (Claycomb et al., 1998). Briefly, HL-1 cells were grown on fibronectin (0.02%) / gelatin (10 μg·ml^{-1}) coated flasks in Claycomb medium supplemented with 10% FBS, 100 μg·ml^{-1} penicillin/streptomycin, 0.1-mM norepinephrine, and 2-mM L-glutamine. Stable knockdown of the endogenous mVDAC2 in HL-1 cardiomyocytes was performed by lentiviral transduction with shLenti2.4G-mVDAC2 or shLenti2.4G-Ctrl as described previously (Subedi et al., 2011) In brief, HL-1 cells were transduced in serum-free Claycomb medium with lentivirus at a multiplicity of infection (MOI) of 30 in the presence of 8 μg·ml^{-1} polybrene. Three days after transduction, cells were selected with 2 μg·ml^{-1} puromycin for 10 days and cultured for additional three passages. For overexpression of zVDAC2 and zVDAC2^{AAA}, transduction was performed as described above using a MOI of 25. After 4 days, nlsEGFP-positive cells were selected by FACS sorting on a BD FACS Aria III.

2.7 | SR-mitochondria Ca^{2+} transfer

Fluorescence-based measurements of mitochondrial Ca^{2+} were performed as previously described (Schweitzer et al., 2017). In brief, HL-1 cells (RRID:CVCL_0303) were plated in 96-well plates 1 day prior to the experiment. To monitor mitochondrial Ca^{2+}, cells were stained with Rhod-2, AM (Thermo Fisher, Darmstadt, Germany) and permeabilized using digitonin. Mitochondrial Ca^{2+} was constantly monitored in a fluorescence plate reader (Infinite® 200 PRO multimode reader, Tecan, Maennedorf, Switzerland), and SR Ca^{2+} release was induced by superfusion with 10-mM caffeine.

2.8 | Metabolic stability assay

Efsevin (10 mM in DMSO) was co-incubated with human liver microsomes at 37°C at an initial concentration of 1 μM. The reaction was initiated by addition of 1-mM NADPH; 0, 5, 10, 30, and 60 minutes after starting the reaction, small aliquots were transferred into ice-cold acetonitrile and centrifuged at 16000× *g* for 10 min. Supernatants were analysed by LC–MS/MS. Experiments were performed as contract research at 3D BioOptima Co., Ltd., Suzhuo, China.

2.9 | Data and statistical analysis

The data and statistical analysis comply with the recommendations of the *British Journal of Pharmacology* on experimental design and analysis in pharmacology (Curtis et al., 2018). zVDAC2 channels were inserted into lipid bilayers and measured before and after addition of efsevin in recording solution, thus leading groups of equal size. In some instances, membranes ruptured during the recording explaining smaller sample size for recordings with efsevin. The recording before efsevin addition served as a control. Since efsevin was the only drug investigated and was added in measuring solution, randomization and blinding were not applied. All traces were equally analysed for predefined parameters like average current or open state to exclude operators bias. For Ca^{2+} uptake experiments on HL-1 cardiomyocytes, wells were randomly assigned to control, efsevin and **ruthenium red** (RuR) group to generate groups of equal size. Wells were microscopically inspected after the experiment, and those in which cells have detached were excluded from the analysis. No data transformation or outlier removal was performed, and all traces were equally analysed for maximum response by a predefined script to exclude operators bias. Since nature and magnitude of the effects of efsevin on zVDAC2 were unknown before the experiment and not predictable, a sample size evaluation was not feasible.

Statistical analysis was only performed for sample sizes >5 from independent experiments (i.e. individual insertions in lipid bilayers, individual runs of computational docking, and individual cultures of HL-1 cardiomyocytes), and the obtained data were used for statistical analysis without normalization and outlier removal. Statistical analysis was performed using Prism 7 (GraphPad Software, San Diego, USA). Data are presented as mean ± *SEM* of *n* individual experiments (no technical replicates). Normality of data was determined by Shapiro–Wilk test. Tests for statistical significance were conducted as indicated and where unpaired student's t-test for comparison of two groups with normal distribution of data, Mann Whitney U test for comparison of two groups with non-normal distribution of data, and Kruskal-Wallis test with Dunn's post hoc test for multigroup comparison with non-normal data distribution. Statistical significance of $P < .05$ is indicated as *.

2.10 | Materials

Efsevin was synthesized as described before (Henry et al., 2014). Protein purification was performed on an Äkta pure, and all Äkta

material was purchased from GE Healthcare, Munich, Germany; LDAO was obtained from VWR, Darmstadt, Germany. The lipid bilayer set-up and all consumables including 1,2-diphytanoyl-sn-glycero-3-phosphatidylcholine (DPhPC) were purchased from Ionovation, Osnabrück, Germany. Ruthenium red and caffeine used for the HL-1 Ca^{2+} uptake assay were purchased from Sigma-Aldrich (Munich, Germany). Plasmids pCCLc-CMV, pCMVΔ8.91 and pCAGGS-VSV-G were obtained as a gift from Dr. Donald Kohn, University of California Los Angeles, USA; plasmid shLenti2.4G-mVDAC2 and shLenti2.4G-Ctrl were generously provided by Dr. Yeon Soo Kim from Inje University, Gimhae, South Korea. HL-1 cardiomyocytes were obtained as a gift from Dr. William Claycomb, Louisiana State University, New Orleans, USA; Claycomb medium and all cell culture supplies were obtained from Sigma-Aldrich (Munich, Germany).

2.11 | Nomenclature of targets and ligands

Key protein targets and ligands in this article are hyperlinked to corresponding entries in http://www.guidetopharmacology.org, the common portal for data from the IUPHAR/BPS Guide to PHARMACOLOGY (Harding et al., 2018), PHARMACOLOGY.

3 | RESULTS

3.1 | Efsevin reduces currents through zVDAC2

Recombinant zVDAC2 protein was purified from *Escherichia coli* as previously described (Schredelseker et al., 2014) and inserted into diphytanoylphosphatidylcholine (DPhPC) planar lipid bilayers. Currents were measured in response to 10 s test pulses to potentials from −60 to +60 mV in 1-M KCl. As shown in Figure 1a, typical average currents of 41 ± 3pA were recorded at 10 mV, where the channel almost exclusively resides in its open state (Colombini, 1989; Schredelseker et al., 2014). VDAC-typical flattening of the current–voltage relationship (*I*–*V* curve) was observed starting at approximately ±30 mV (Figure 1b), where the channel starts gating until finally being preferentially in its closed state at potentials above +50 mV or below −50 mV (Figure 1a,b). The observed *I*–*V* curve for zVDAC2 translates into a bell-shaped conductance–voltage

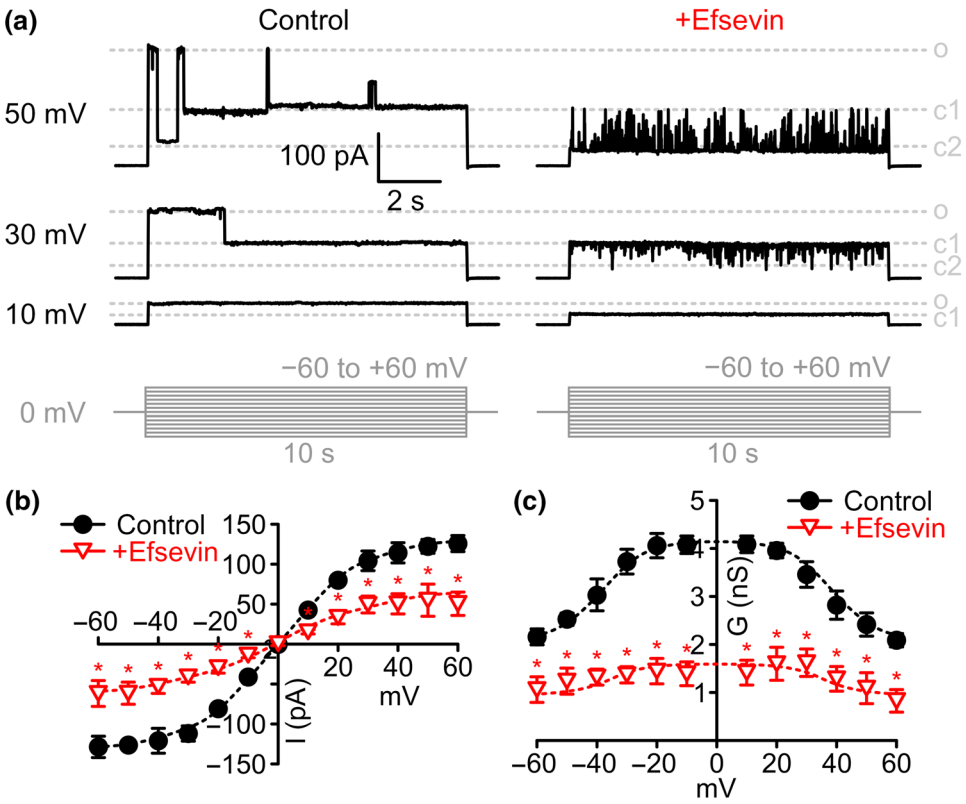

FIGURE 1 Effects of efsevin on zVDAC2 currents in planar lipid bilayers. (a) Typical current recordings from zVDAC2 inserted into painted planar DPhPC lipid bilayers in 1-M KCl in response to 10 s test pulses from 0 to 10, 40, and 50 mV, respectively, under control conditions (left) and after addition of 8-μM efsevin (right) to the same channel. Gating between three major states open (o), closed1 (c1) and closed2 (c2) and few subconductance states can be observed (pulse protocol in shown in grey). (b) Current–voltage relationship of average zVDAC2 currents before (*n* = 9 individual channels, black circles) and after addition of efsevin (*n* = 6 individual channels, red triangles, Unpaired Student's *t*-test). (c) Conductance–voltage relationship of zVDAC2 before (*n* = 9 individual channels, black circles) and after addition of efsevin (*n* = 6 individual channels, red triangles, Unpaired Student's *t*-test)

relationship that is characteristic of VDACs (Figure 1c). Strikingly, addition of 8-μM efsevin destabilized the channel's high conductance state and dramatically reduced currents through zVDAC2 by about 50% across all voltages.

3.2 | Efsevin reduces zVDAC2 open probability and shifts the channel towards closed states

Since efsevin profoundly reduced average zVDAC2 conductance, we further analysed the biophysical properties of zVDAC2 single channel currents to dissect the effects of efsevin on single channel conductance versus open probability of the channel. VDAC has been shown to undergo voltage-dependent gating between an anion-selective high-conductance state, referred to as the classical open state and several cation-selective low-conductance states, referred to as closed states (Colombini, 1989; Guardiani et al., 2018; Menzel et al., 2009; Mertins et al., 2012). Under control conditions, we observed gating of the channel between the classical open state with a conductance 4.2 ± 0.2 ns and two closed states with conductances of 2.0 ± 0.1 ns for closed state 1 and 1.2 ± 0.04 ns for closed state 2 (Figure 2a,b). Efsevin shifts the channel mainly into closed states 1 and 2 with only a few scarce openings of the channel into the open state, already at low potentials. Conductances of the three states remained comparable to control conditions (open: 4.1 ± 0.1 ns; closed1: 2.1 ± 0.2 ns; closed2: 1.0 ± 0.04 ns; Figure 2b). The shift towards the closed states becomes most obvious when plotting the open probability (P_O) of the channel against voltage (Figure 2c). Interestingly, at the physiologically relevant low potentials of ±30 mV (Lemeshko, 2006; Porcelli et al., 2005), the apo-form of the channel resides mainly in the open state, while the efsevin-bound form is preferentially closed (Figure 2d). The VDAC closed states were previously defined as more cation-selective compared to the open state (Tan & Colombini, 2007; Zachariae et al., 2012). We therefore measured the ion selectivity of the dominant states, the open

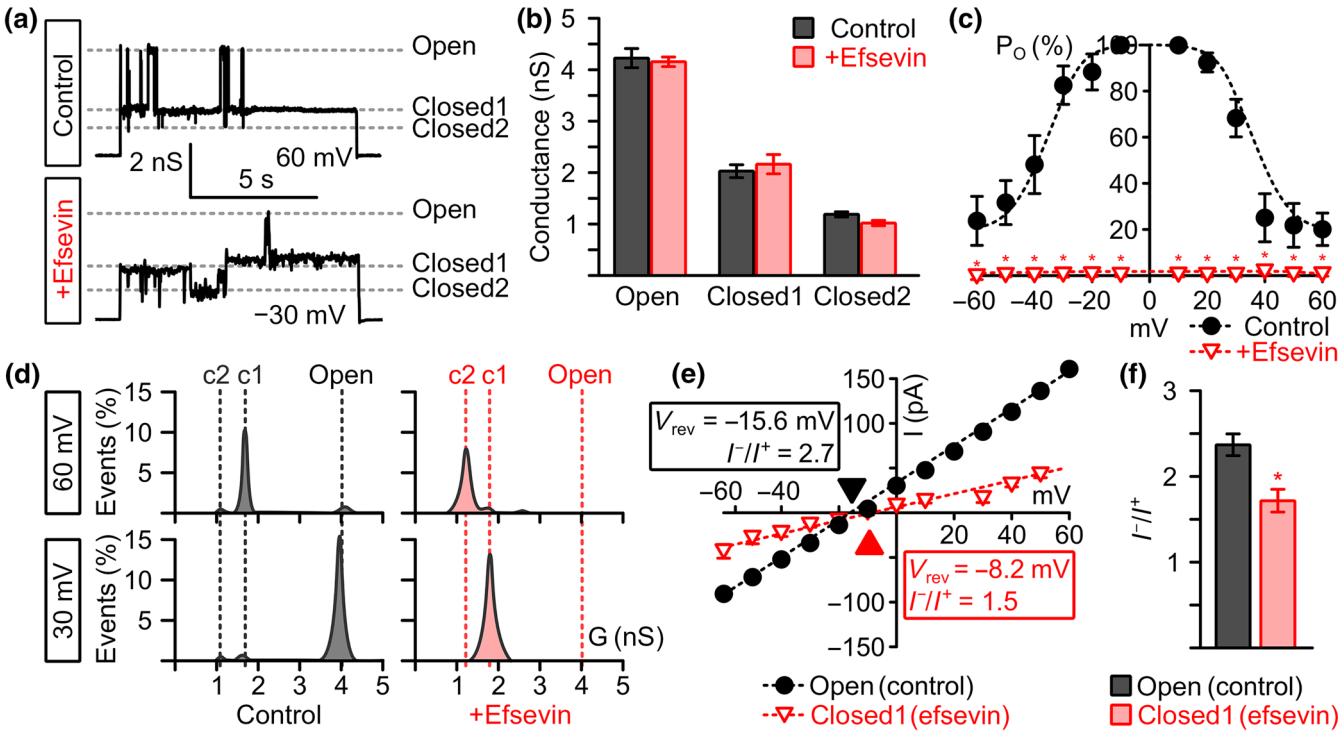

FIGURE 2 Effects of efsevin on zVDAC2 conductance and open probability (P_O). (a) Representative recordings of zVDAC2 in a painted lipid bilayer under control conditions (upper trace) and after addition of 8-μM efsevin (lower trace) at potentials where typical gating behaviour between the three states is observed, that is, very low/high potentials under control conditions and moderate potentials after addition of efsevin. Currents through the open and two distinct closed states of the channel are indicated by dashed lines. (b) Addition of 8-μM efsevin does not change the conductance of the three distinct conductance states of zVDAC2 (n = 12 individual channels for control and 6 individual channels after addition of efsevin). (c) Analysis of the open probability (P_O) of zVDAC2 shows a significant shift of the channel towards the closed states across all voltages after addition of efsevin (n = 12 for control and n = 6 for efsevin, Mann–Whitney U test). (d) Representative conductance histograms from recordings of zVDAC2 with and without efsevin at 30 mV and 60 mV show a shift of the channel from the classical open state to the closed states. (e,f) Current–voltage plots for the open and the efsevin-induced closed state 1 obtained from zVDAC2 in a folded lipid bilayer using a 0.2-M to 1-M KCl gradient reveal a shift in the reversal potential (V_{rev}). (f) Quantitative analysis of selectivity measurements reveals a significant reduction in anion selectivity for the efsevin-induced closed state 1 (n = 6 for control, n = 5 for efsevin, Unpaired Student's t- test)

state of the apo-form and closed state 1 of the efsevin-bound channel using salt gradient conditions (0.2-M [cis] vs. 1-M [trans] KCl) and found a change in the Cl^- to K^+ permeability ratio I^-/I^+ from 2.38 ± 0.13 for the open state to 1.71 ± 0.14 for the efsevin-bound closed state 1 (Figure 2e,f). In conclusion, our data indicate that efsevin binding facilitates channel closure and induces a shift of zVDAC2 towards the less anion-selective low conductance states.

3.3 | Molecular docking reveals an efsevin binding site between the inner channel wall and the pore-lining N-terminal α-helix

To identify the interaction between efsevin and zVDAC2 at the molecular level, we performed protein-ligand docking using AutoDock Vina (Trott & Olson, 2010). By docking the flexible form of efsevin into the rigid crystal structure of zVDAC2 (Schredelseker et al., 2014), a binding pocket formed between the inner channel wall and the N-terminal α-helix of zVDAC2 repeatedly showed the lowest binding energies in 15 independent dockings yielding 135 conformations (Figures 3a and S1). To further investigate molecular interactions between zVDAC2 and efsevin within this pocket, we performed subsequent docking simulations in which residues facing this binding site were made flexible. We identified multiple conformations with binding affinities below −8.0 kcal·mol^{-1} in which the dihydropyrrole of the efsevin core with the ethoxycarbonyl and phenyl substituents was always interacting with residues in the channel wall, while the *p*-tolyl substituent of the sulphonamide group faces the lumen of the pore and interacts with the hinge region of the N-terminal α-helix. Interactions of efsevin with zVDAC2 were identified with residues F18, N19, Y22, G23, F24 and M26 in the N-terminal α-helix and with residues N207, L208, A209, R218, F219, G220, K236, V237, N238, L242, G244 and L262 in the β-barrel, whereof asparagine 207, lysine 236 and asparagine 238 were the most prominent interaction partners. Hydrogen bonds and hydrophobic interactions with these three amino acids were present in the majority of conformations (Figure 3b). Figure 3c,d shows one representative conformation in which efsevin is held in place by N207, K236 and N238 in the channel wall and interacts with the α-helix through hydrophobic interactions with residues F18, N19, Y22, G23 and F24. To finally investigate translatability of the docking results to the human channel, we created

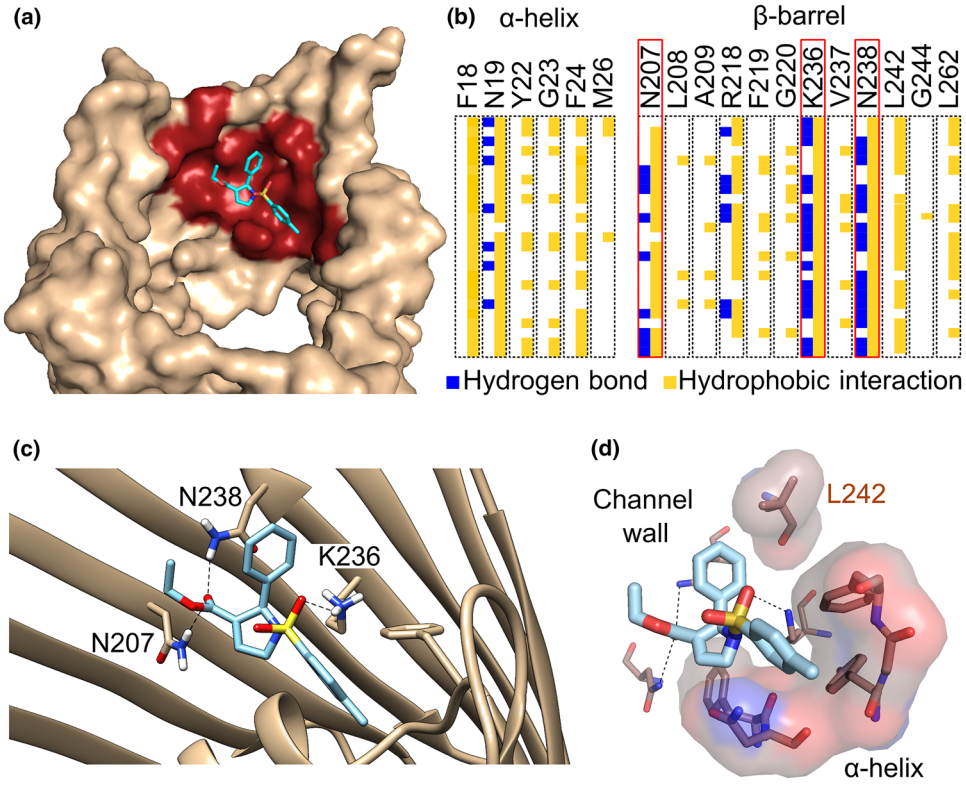

FIGURE 3 Predicted binding site of efsevin on zVDAC2 obtained by molecular docking. (a) Side view of the channel (pdb: 4bum, light brown) displays a binding pocket (red) for efsevin (light blue) located in the interspace between the inner channel wall and the N-terminal pore-lining α-helix. (b) Analysis of 25 different molecular dockings (rows) reveals interactions between efsevin and 18 amino acid rests of zVDAC2 (columns) through hydrogen bonds (blue) and hydrophobic interactions (yellow). Residues with the most interactions (N207 in β-sheet 14, K236, and N238 in β-sheet 16 of the barrel) are boxed in red. (c) Detailed view of one representative docking with efsevin binding to the channel through hydrogen bonds between the most prominent amino acids highlighted in (b) and efsevin. (d) Surface representation of residues forming hydrophobic interactions in the conformation shown in (c) reveals a cavity that accommodates the *p*-tolyl group of efsevin on the hinge of the flexible N-terminal α-helix. Nitrogen is shown in blue, oxygen in red, and sulfur in yellow

a model of human VDAC2 (hVDAC2) by homology modelling using SWISS-MODEL (Waterhouse et al., 2018) since no experimentally determined structure for hVDAC2 is currently available. In eight out of 10 independent docking experiments, the conformation with the lowest binding energy was found in the same binding pocket like in zVDAC2 indicating that this binding pocket is conserved among species (Figure S2).

3.4 | Elimination of residues N207, K236 and N238 abolishes the efsevin sensitivity of zVDAC2

To confirm the predicted efsevin binding site by mutational analysis, we created a zVDAC2 mutant in which residues N207, K236 and N238 were substituted by alanine residues, zVDAC2$^{N207A/K236A/N238A}$ (zVDAC2^{AAA}). Lipid bilayer recordings of this mutant showed that it forms a functional channel with a similar conductance–voltage relationship, single channel conductance and P_O compared to wild-type zVDAC2 (Figure S3). Most strikingly however, the channel was insensitive to efsevin, demonstrated by comparable values for the conductance–voltage relationship, single channel conductance and P_O before and after addition of efsevin (Figure 4).

3.5 | Efsevin mediates SR-mitochondria Ca^{2+} transfer by binding to the N207/K236/N238 binding site

To evaluate if the observed efsevin-induced electrophysiological changes can explain the enhanced mitochondrial Ca^{2+} uptake observed previously for HeLa cells and HL-1 cardiomyocytes (Schweitzer et al., 2017; Shimizu et al., 2015), we developed a heterologous expression system for zVDAC2. To this aim, we created a stable HL-1 cardiomyocyte line in which the endogenous mouse VDAC2 (mVDAC2) was knocked down by stable expression of shRNA (Subedi et al., 2011; Figure S4) and overexpressed shRNA-insensitive zVDAC2 constructs by lentiviral transduction. Ca^{2+} uptake into mitochondria upon caffeine-induced Ca^{2+} release from the sarcoplasmic reticulum (SR) was then measured in permeabilized Rhod-2 stained cells (Figure 5). In line with previous experiments, knock-down of the endogenous mVDAC2 eliminated transfer of Ca^{2+} from the sarcoplasmic reticulum into mitochondria (Subedi et al., 2011). While wild-type HL-1 cardiomyocytes displayed maximum $\Delta F/F_0$ values of 0.14 ± 0.02 that were enhanced to 0.38 ± 0.03 by 10-μM efsevin, shRNA-expressing cells displayed $\Delta F/F_{0\ max}$ values of 0.04 ± 0.03, which were indistinguishable from those obtained from cells treated with the mitochondrial Ca^{2+} uptake blocker ruthenium red (RuR; $\Delta F/F_{0\ max}$ = 0.06 ± 0.02) or efsevin ($\Delta F/F_{0\ max}$ = 0.06 ± 0.01, not significant). Though lack of VDAC2 was previously described to induce apoptosis and we can thus not rule out downstream effects induced by mVDAC2 knock down in these cells, the shmVDAC2 cell line was stable for the time of our experiments and thus suitable for heterologous overexpression experiments. Overexpression of zVDAC2 completely restored sarcoplasmic reticulum-mitochondria Ca^{2+} transfer to $\Delta F/F_{0\ max}$ = 0.14 ± 0.02, which was sensitive to modulation by efsevin ($\Delta F/F_{0\ max}$ = 0.34 ± 0.02). Strikingly, zVDAC2^{AAA} likewise restored mitochondrial Ca^{2+} uptake to levels indistinguishable from wild-type zVDAC2 ($\Delta F/F_{0\ max}$ = 0.15 ± 0.02) but was insensitive to treatment with efsevin ($\Delta F/F_{0\ max}$ = 0.16 ± 0.02). These data strongly indicate that the efsevin induced changes in zVDAC2 electrophysiology account for the enhanced mitochondrial Ca^{2+} uptake in cardiomyocytes.

4 | DISCUSSION

Here, we describe the efsevin–zVDAC2 interaction at a biophysical and structural level. Efsevin was previously shown to enhance mitochondrial Ca^{2+} uptake and to be a powerful modulator of cardiac rhythmicity and a potent suppressor of cardiac arrhythmia. Efsevin suppresses arrhythmogenesis in both, models for Ca^{2+} overload and models for inherited arrhythmias like catecholaminergic polymorphic

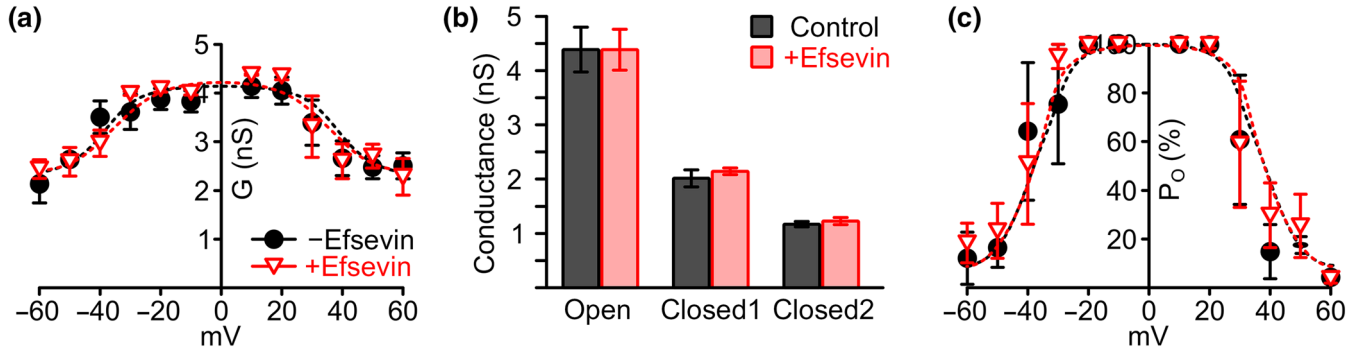

FIGURE 4 Effects of efsevin on conductance, and open probability (P_O) of zVDAC2^{AAA} in lipid bilayers. (a) Conductance–voltage relation of zVDAC2^{AAA} in painted bilayer recordings reveals a comparable shape before and after addition of 8-μM efsevin. (b) No differences in single channel conductance for open and closed states of zVDAC2^{AAA} were observed after addition of efsevin. (c) Finally, in zVDAC2^{AAA}, efsevin was unable to induce the reduction of P_O observed for wild-type zVDAC2 (*n* = 4 individual channels for control and 3 individual channels after addition of efsevin)

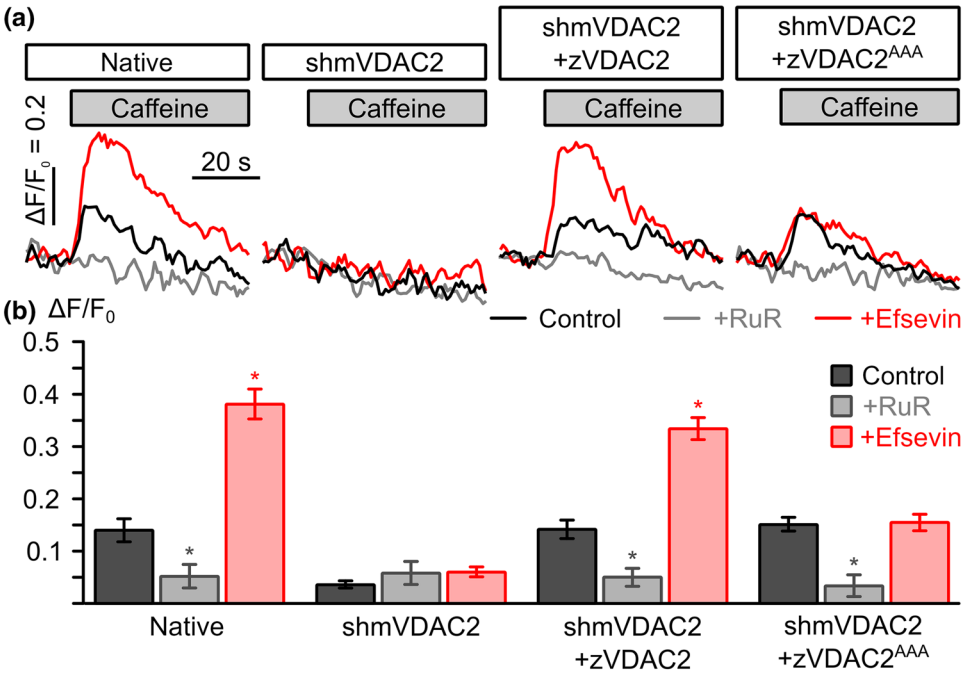

FIGURE 5 Sarcoplasmic reticulum (SR)-mitochondria Ca^{2+} transfer upon heterologous expression of zVDAC2 and zVDAC2^{AAA} in HL-1 cardiomyocytes. (a) Representative recordings of mitochondrial Ca^{2+} upon application of 10-mM caffeine to induce SR calcium release from permeabilized HL-1 cardiomyocytes. Traces from control conditions (black), recordings in the presence of 10-μM ruthenium red to block mitochondrial Ca^{2+} uptake (RuR, grey) and in the presence of 10-μM efsevin (red) are shown for native HL-1 cells (native), cells transduced with shRNA targeting the endogenous mouse mVDAC2 (shmVDAC2), and cells overexpressing zVDAC2 and zVDAC2^{AAA}, respectively. (b) Statistical analysis of SR-mitochondria Ca^{2+} transfer experiments. While native HL-1 cardiomyocytes showed an efsevin-sensitive uptake of Ca^{2+} into mitochondria (n = 21 for control, n = 7 for RuR, and n = 18 for efsevin), this uptake was abolished upon knock-down of the endogenous mVDAC2 (shmVDAC2, n = 24 for control, n = 8 for RuR, n = 15 for efsevin). Subsequent heterologous expression of zVDAC2 (shmVDAC2, n = 21 for control, n = 7 for RuR, n = 15 for efsevin) and zVDAC2^{AAA} (shmVDAC2^{AAA}, n = 18 for control, n = 6 for RuR, n = 18 for efsevin) revealed restoration of SR-mitochondria Ca^{2+} transfer. However, only zVDAC2 but not zVDAC2^{AAA} was sensitive to efsevin (Kruskal–Wallis test with Dunn's post hoc test)

ventricular tachycardia. In a murine model for CPVT, efsevin significantly reduced episodes of ventricular tachycardia, while no adverse effects of efsevin were observed after up to 8 days of continuous treatment. VDAC2, which was previously described as an essential component of the mitochondrial Ca^{2+} uptake machinery of the heart (Subedi et al., 2011), was identified as the primary target of efsevin (Shimizu et al., 2015). These findings make VDAC2-mediated mitochondrial Ca^{2+} uptake a promising therapeutic target for the development of a novel class of antiarrhythmic drugs with efsevin as a lead candidate. However, efsevin was identified in a chemical screen using 168 newly synthesized diversity-oriented compounds (Shimizu et al., 2015) without further compound optimization. In our HL-1-based sarcoplasmic reticulum-mitochondria Ca^{2+} transfer assay, efsevin showed a half-maximal activity at 2.2 μM (Figure S5A). Preliminary results on efsevin's pharmacokinetics show that it is hydrolysed rapidly in liver microsomes (Figure S5B). Furthermore, binding of efsevin to other targets, including VDAC isoforms 1 and 3, was never tested. Thus, its unknown selectivity, the low stability of efsevin and the relatively high EC_{50} value indicate the need for chemical optimization of the compound before further preclinical and clinical studies are performed. In this study, we present a molecular model of the efsevin binding site on zVDAC2 and thereby provide a basis for structure-based drug optimization in future experiments.

When discussing VDAC2 as a potential drug target for cardiac arrhythmia, it should be noted that the transfer of Ca^{2+} from the sarcoplasmic reticulum into mitochondria is most likely a specialized role of VDAC2 in cardiomyocytes, presumably accomplished by a functional or even physical coupling to the ryanodine receptor (Min et al., 2012; Shimizu et al., 2015; Subedi et al., 2011) and might be less relevant or maybe accomplished by other VDAC isoforms in other cell types. In fact, VDAC1 was previously reported to promote Ca^{2+} transfer from the endoplasmic reticulum into mitochondria in non-excitable cells through coupling to the **IP_3 receptor** (De Stefani et al., 2012; Rapizzi et al., 2002; Szabadkai et al., 2006). It is thus conceivable that despite the ubiquitous expression of VDACs in the body, efsevin-mediated effects are most pronounced or even limited to cardiomyocytes due to the specialized role of VDAC2 in this tissue. This effect might also explain the lack of major side effects that were observed previously in translational models (Schweitzer et al., 2017). However, future studies are needed to evaluate the role of the efsevin-mediated effects on other VDAC2-mediated effects like

apoptosis or regulation of bioenergetics (for a review, see Naghdi & Hajnóczky, 2016). Furthermore, although VDAC2 was identified as the primary target of efsevin and efsevin-induced antiarrhythmic effects were shown to depend on VDAC2 (Shimizu et al., 2015), interaction of efsevin with other VDAC isoforms were never investigated. Given a high sequence conservation of the residues involved in VDAC2 binding identified in this study, it is conceivable that efsevin binds to VDAC isoforms 1 and 3. This effect might be less relevant during short-term treatment of mice and fish but might have long-term impacts on, for example, bioenergetics and thus needs to be investigated in future studies.

Using computational docking on the crystal structure of zVDAC2, we identified a binding pocket formed by the inner channel wall and the N-terminal helix. The putative binding site was confirmed by replacing three prominent residues inside the pocket by alanines which resulted in insensitivity of the channel to efsevin in lipid bilayers. It is of note that we used a C-terminal His_6-tag for purification of the channel for subsequent bilayer experiments which is not present in the structure used for computational docking. It is thus conceivable that the His_6-tag interferes with efsevin and promotes effects seen in bilayer experiments. However, the His_6-tag is located approximately 25 Å away from the proposed binding site on the opposed mouth of the channel making interference unlikely. Furthermore, we evaluated the proposed binding site by heterologous expression of zVDAC2 without the C-terminal His_6-tag in HL-1 cardiomyocytes and found that efsevin sensitivity of the channel was again promoted through the proposed binding site. To prove translatability of the results obtained from zVDAC2, we created a homology model of hVDAC2 using zVDAC2 as a template and found that the lowest bind energy was calculated in the same pocket in eight out of 10 individual docking experiments. The mammalian channel includes additional 11 amino acids on the N-terminus of the channel. Unfortunately, no homologous structures of this additional sequence have been resolved so far, and coordinates for homology modelling are missing. It is thus again conceivable that the additional N-terminus in mammalian channels could interfere with efsevin binding. However, in HL-1 cardiomyocytes, we observe very similar effects of efsevin on native cells expressing the endogenous mVDAC2, which includes the N-terminal extension and heterologously expressed zVDAC2. Although these data do not rule out the possibility that efsevin promotes its effects on the two distinct channels differently, it argues against it.

Our data indicate that efsevin binds to the inner wall of the β-barrel in close proximity to the N-terminal α-helix and thereby affects channel conductance and gating. Although still not fully resolved, various models were proposed to explain gating of VDACs. Almost all models include a role of the N-terminal α-helix ranging from relatively small movements of the helix inside the barrel (Mertins et al., 2012; Shuvo, Ferens, & Court, 2016) to a large movement that place the helix outside of the barrel, which then collapses to induce channel closure (Choudhary et al., 2010; Zachariae et al., 2012). Furthermore, a fixation of the helix inside the pore through disulfate bridges was reported as a possible mechanism to regulate channel gating by redox sensing (Okazaki et al., 2015; Reina et al., 2016). Our data identified a binding pocket for efsevin located in a groove between the N-terminal α-helix and the inner channel wall. In all our predicted binding conformations, efsevin is bound to the channel wall through hydrogen bonds provided by N19, N207, R218, K236 or N238 plus additional hydrophobic interactions and interacts with a binding pocket located on the hinge of the α-helix. Interestingly, one of the residues in the channel wall, K236, was previously reported to form a hydrogen bond with F18 in the α-helix (Ujwal et al., 2008), a residue that interacts with efsevin upon efsevin binding. It is thus conceivable that efsevin interferes with the interaction between the barrel and the helix in zVDAC2 and consequently affects the movement of the α-helix required to modulate the channel. However, it should be noted that the binding of efsevin might induce a conformational change in the channel, which is not considered in our docking model. Further experimental and computational investigations, like molecular dynamics simulations and determination of the ligand-bound VDAC2 structure are thus needed to clarify the exact mode of gating and ion conduction through the channel in the presence and absence of efsevin.

Using an electrophysiological approach, we found efsevin-promoted gating of zVDAC2. Already at low potentials, the channel preferentially gates into the two closed states and only rarely returns to the open state. We demonstrate that the efsevin-induced low conducting states display less anion selectivity compared to the open state which translates into a higher Ca^{2+} flux and consequently into higher Ca^{2+} uptake into mitochondria in cardiomyocytes. This is in line with previous experimental (Tan & Colombini, 2007) and computational (Zachariae et al., 2012) studies, which have shown the closed states of VDAC to be more cation-selective. The observed shift from the open to the closed states is especially relevant at low potentials ranging from −40 to +40 mV. Though it is still under debate whether a membrane potential difference exists over the outer mitochondrial membrane, modelling data suggest a potential of approximately −20 to −27 mV (Lemeshko, 2006) and a study based on pH measurements suggests a potential of approximately −40 mV (Porcelli et al., 2005). This most likely explains the enhanced Ca^{2+} uptake into mitochondria seen in the presence of efsevin. The data presented in this study are thus in agreement with the concept of increased Ca^{2+} flux upon channel closure.

In this study, we present a binding pocket in zVDAC2 and an associated biophysical mechanism, namely, a modification of voltage gating and a shift towards the cation-selective closed states. VDACs were previously suggested as promising drug targets mainly because of their prominent role in apoptosis (for a review, see Magrì, Reina, & De Pinto, 2018). However, it remained unclear whether the role of VDAC in apoptosis was directly associated with the channel's gating behaviour or rather with a modified interaction with partner proteins such as hexokinase or members of the Bcl-2 family. In this study, we present evidence that the efsevin-induced change in gating facilitates transfer of Ca^{2+} from the SR into mitochondria. Interestingly, we never observed an involvement of the drug in apoptosis, neither in this study nor in previous studies (Schweitzer et al., 2017; Shimizu et al., 2015) despite a previously identified isoform-specific role for

VDAC2 in apoptosis through recruitment of Bax (Lauterwasser et al., 2016; Ma et al., 2014). Efsevin could thus serve as a tool to dissect these functions in future studies.

Taken together, we provide functional and structural data that explains the interaction between zVDAC2 and its modulator efsevin on a molecular basis. Our data provide new insights into VDAC2 function as well as a basis for computer-aided design of optimized compounds that could serve as research compounds and therapeutics for cardiac arrhythmia.

ACKNOWLEDGEMENTS

We would like to thank Brigitte Mayerhofer for technical assistance and Tatiana Rostovtseva and Anna Krautloher for help with data analysis. We thank Michael Hristov from the FACS core facility at the Institute for Cardiovascular Prevention at LMU Munich for performing FACS sorting of HL-1 cardiomyocytes. This work was supported by the Deutsche Forschungsgesellschaft DFG SCHR 1471/1-1 to J.S. and the U.S. National Institute of Health grant R01GM071779 to O.K.

CONFLICT OF INTEREST

The authors declare no conflicts of interest.

AUTHOR CONTRIBUTIONS

J.S. and T.G. conceptualized the study and acquired funding. F.W. and J.S. performed bilayer recordings and mitochondrial Ca^{2+} uptake experiments and analysed results. P.G. performed and analysed ion selectivity recordings. R.K. and A.S. performed molecular docking experiments. O.K. and N.J.D. synthesized efsevin. A.N. analysed data. J.S. wrote the manuscript. All authors commented on the manuscript.

DECLARATION OF TRANSPARENCY AND SCIENTIFIC RIGOUR

This Declaration acknowledges that this paper adheres to the principles for transparent reporting and scientific rigour of preclinical research as stated in the *BJP* guidelines for Design & Analysis, and as recommended by funding agencies, publishers and other organisations engaged with supporting research.

ORCID

Robin Kopp https://orcid.org/0000-0002-1639-2868

Johann Schredelseker https://orcid.org/0000-0002-6657-0466

REFERENCES

Benjamin, E. J., Virani, S. S., Callaway, C. W., Chamberlain, A. M., Chang, A. R., Cheng, S., … American Heart Association Council on Epidemiology and Prevention Statistics Committee and Stroke Statistics Subcommittee. (2018). Heart disease and stroke statistics—2018 update: A report from the American Heart Association. *Circulation*, *137*, e67–e492. https://doi.org/10.1161/CIR.0000000000000558

Cheng, E. H. Y., Sheiko, T. V., Fisher, J. K., Craigen, W. J., & Korsmeyer, S. J. (2003). VDAC2 inhibits BAK activation and mitochondrial apoptosis. *Science*, *301*, 513–517. https://doi.org/10.1126/science.1083995

Choudhary, O. P., Ujwal, R., Kowallis, W., Coalson, R., Abramson, J., & Grabe, M. (2010). The electrostatics of VDAC: Implications for selectivity and gating. *Journal of Molecular Biology*, *396*, 580–592. https://doi.org/10.1016/j.jmb.2009.12.006

Claycomb, W. C., Lanson, N. A., Stallworth, B. S., Egeland, D. B., Delcarpio, J. B., Bahinski, A., & Izzo, N. J. (1998). HL-1 cells: A cardiac muscle cell line that contracts and retains phenotypic characteristics of the adult cardiomyocyte. *Proceedings of the National Academy of Sciences of the United States of America*, *95*, 2979–2984. https://doi.org/10.1073/pnas.95.6.2979

Colombini, M. (1989). Voltage gating in the mitochondrial channel, VDAC. *Journal of Membrane Biology*, *111*, 103–111. https://doi.org/10.1007/bf01871775

Curtis, M. J., Alexander, S., Cirino, G., Docherty, J. R., George, C. H., Giembycz, M. A., … Ahluwalia, A. (2018). Experimental design and analysis and their reporting II: Updated and simplified guidance for authors and peer reviewers. *British Journal of Pharmacology*, *175*, 987–993. https://doi.org/10.1111/bph.14153

De Stefani, D., Bononi, A., Romagnoli, A., Messina, A., De Pinto, V., Pinton, P., & Rizzuto, R. (2012). VDAC1 selectively transfers apoptotic Ca^{2+} signals to mitochondria. *Cell Death and Differentiation*, *19*, 267–273. https://doi.org/10.1038/cdd.2011.92

Ebert, A. M., Hume, G. L., Warren, K. S., Cook, N. P., Burns, C. G., Mohideen, M. A., … Garrity, D. M. (2005). Calcium extrusion is critical for cardiac morphogenesis and rhythm in embryonic zebrafish hearts. *Proceedings of the National Academy of Sciences of the United States of America*, *102*, 17705–17710. https://doi.org/10.1073/pnas.0502683102

Guardiani, C., Magrì, A., Karachitos, A., Di Rosa, M. C., Reina, S., Bodrenko, I., … De Pinto, V. (2018). yVDAC2, the second mitochondrial porin isoform of *Saccharomyces cerevisiae*. *Biochimica et Biophysica Acta, Bioenergetics*, *1859*, 270–279. https://doi.org/10.1016/j.bbabio.2018.01.008

Harding, S. D., Sharman, J. L., Faccenda, E., Southan, C., Pawson, A. J., Ireland, S., … NC-IUPHAR. (2018). The IUPHAR/BPS Guide to pharmacology in 2018: Updates and expansion to encompass the new guide to immunopharmacology. *Nucleic Acids Research*, *46*, D1091–D1106. https://doi.org/10.1093/nar/gkx1121

Henry, C. E., Xu, Q., Fan, Y. C., Martin, T. J., Belding, L., Dudding, T., & Kwon, O. (2014). Hydroxyproline-derived pseudoenantiomeric [2.2.1] bicyclic phosphines: Asymmetric synthesis of (+)- and (–)-pyrrolines. *Journal of the American Chemical Society*, *136*, 11890–11893. https://doi.org/10.1021/ja505592h

Hille, B. (2001). *Ion channels of excitable membranes*. Sunderland, MA, USA: Sinauer Associates Inc.

Kirichok, Y., Krapivinsky, G. & Clapham, D. (2004). The mitochondrial calcium uniporter is a highly selective ion channel. *Nature*, *427*, 360–364.

Kwan, K. M., Fujimoto, E., Grabher, C., Mangum, B. D., Hardy, M. E., Campbell, D. S., … Chien, C. B. (2007). The Tol2kit: A multisite gateway-based construction kit for Tol2 transposon transgenesis constructs. *Developmental Dynamics*, *236*, 3088–3099. https://doi.org/10.1002/dvdy.21343

Langenbacher, A. D., Dong, Y., Shu, X., Choi, J., Nicoll, D. A., Goldhaber, J. I., … Chen, J. N. (2005). Mutation in sodium-calcium exchanger 1 (NCX1) causes cardiac fibrillation in zebrafish. *Proceedings of the National Academy of Sciences of the United States of America*, *102*, 17699–17704. https://doi.org/10.1073/pnas.0502679102

Laskowski, R. A., & Swindells, M. B. (2011). LigPlot+: Multiple ligand–protein interaction diagrams for drug discovery. *Journal of Chemical Information and Modeling*, *51*, 2778–2786. https://doi.org/10.1021/ci200227u

Lauterwasser, J., Todt, F., Zerbes, R. M., Nguyen, T. N., Craigen, W., Lazarou, M., … Edlich, F. (2016). The porin VDAC2 is the mitochondrial platform for Bax retrotranslocation. *Scientific Reports*, *6*, 32994. https://doi.org/10.1038/srep32994

Lemeshko, V. V. (2006). Theoretical evaluation of a possible nature of the outer membrane potential of mitochondria. *European Biophysics Journal*, *36*, 57–66. https://doi.org/10.1007/s00249-006-0101-7

Lide, D. R. (2006). *CRC handbook of chemistry and physics* (87th ed.). Boca Raton: CRC Press, Taylor & Francis Group.

Ma, S. B., Nguyen, T. N., Tan, I., Ninnis, R., Iyer, S., Stroud, D. A., … Dewson, G. (2014). Bax targets mitochondria by distinct mechanisms before or during apoptotic cell death: a requirement for VDAC2 or Bak for efficient Bax apoptotic function. *Cell Death and Differentiation*, *21*, 1925–1935. https://doi.org/10.1038/cdd.2014.119

Magrì, A., Reina, S., & De Pinto, V. (2018). VDAC1 as pharmacological target in cancer and neurodegeneration: Focus on its role in apoptosis. *Frontiers in Chemistry*, *6*, 108.

Menzel, V. A., Cassará, M. C., Benz, R., De Pinto, V., Messina, A., Cunsolo, V., … Hinsch, E. (2009). Molecular and functional characterization of VDAC2 purified from mammal spermatozoa. *Bioscience Reports*, *29*, 351–362. https://doi.org/10.1042/BSR20080123

Mertins, B., Psakis, G., Grosse, W., Back, K. C., Salisowski, A., Reiss, P., … Essen, L. O. (2012). Flexibility of the N-terminal mVDAC1 segment controls the channel's gating behavior. *PLoS ONE*, *7*, e47938. https://doi.org/10.1371/journal.pone.0047938

Min, C. K., Yeom, D. R., Lee, K.-E., Kwon, H.-K., Kang, M., Kim, Y.-S., … Kim, D. H. (2012). Coupling of ryanodine receptor 2 and voltage-dependent anion channel 2 is essential for Ca^{2+} transfer from the sarcoplasmic reticulum to the mitochondria in the heart. *The Biochemical Journal*, *447*, 371–379. https://doi.org/10.1042/BJ20120705

Morris, G. M., Huey, R., Lindstrom, W., Sanner, M. F., Belew, R. K., Goodsell, D. S., & Olson, A. J. (2009). AutoDock4 and AutoDockTools4: Automated docking with selective receptor flexibility. *Journal of Computational Chemistry*, *30*, 2785–2791. https://doi.org/10.1002/jcc.21256

Naghdi, S., & Hajnóczky, G. (2016). VDAC2-specific cellular functions and the underlying structure. *Biochimica et Biophysica Acta, Molecular Cell Research*, *1863*, 2503–2514. https://doi.org/10.1016/j.bbamcr.2016.04.020

Okazaki, M., Kurabayashi, K., Asanuma, M., Saito, Y., Dodo, K., & Sodeoka, M. (2015). VDAC3 gating is activated by suppression of disulfide-bond formation between the N-terminal region and the bottom of the pore. *Biochimica et Biophysica Acta (BBA)-Biomembranes*, *1848*, 3188–3196.

Porcelli, A. M., Ghelli, A., Zanna, C., Pinton, P., Rizzuto, R., & Rugolo, M. (2005). pH difference across the outer mitochondrial membrane measured with a green fluorescent protein mutant. *Biochemical and Biophysical Research Communications*, *326*, 799–804. https://doi.org/10.1016/j.bbrc.2004.11.105

Raghavan, A., Sheiko, T. V., Graham, B. H., & Craigen, W. J. (2012). Voltage-dependant anion channels: Novel insights into isoform function through genetic models. *Biochimica et Biophysica Acta-Biomembranes*, *1818*, 1477–1485. https://doi.org/10.1016/j.bbamem.2011.10.019

Rapizzi, E., Pinton, P., Szabadkai, G., Wieckowski, M. R., Vandecasteele, G., Baird, G., … Rizzuto, R. (2002). Recombinant expression of the voltage-dependent anion channel enhances the transfer of Ca^{2+} microdomains to mitochondria. *The Journal of Cell Biology*, *159*, 613–624. https://doi.org/10.1083/jcb.200205091

Reina, S., Checchetto, V., Saletti, R., Gupta, A., Chaturvedi, D., Guardiani, C., … de Pinto, V. (2016). VDAC3 as a sensor of oxidative state of the intermembrane space of mitochondria: The putative role of cysteine residue modifications. *Oncotarget*, *7*, 2249–2268. https://doi.org/10.18632/oncotarget.6850

Rostovtseva, T. K., Gurnev, P. A., Chen, M.-Y., & Bezrukov, S. M. (2012). Membrane lipid composition regulates tubulin interaction with mitochondrial voltage-dependent anion channel. *The Journal of Biological Chemistry*, *287*, 29589–29598. https://doi.org/10.1074/jbc.M112.378778

Schredelseker, J., Paz, A., López, C. J., Altenbach, C., Leung, C. S., Drexler, M. K., … Abramson, J. (2014). High-resolution structure and double electron-electron resonance of the zebrafish voltage dependent anion channel 2 reveal an oligomeric population. *The Journal of Biological Chemistry*, *289*, 12566–12577. https://doi.org/10.1074/jbc.M113.497438

Schweitzer, M. K., Wilting, F., Sedej, S., Dreizehnter, L., Dupper, N. J., Tian, Q., … Schredelseker, J. (2017). Suppression of arrhythmia by enhancing mitochondrial Ca^{2+} uptake in catecholaminergic ventricular tachycardia models. *JACC Basic to Translational Science*, *2*, 737–746. https://doi.org/10.1016/j.jacbts.2017.06.008

Shimizu, H., Schredelseker, J., Huang, J., Lu, K., Naghdi, S., Lu, F., … Chen, J. N. (2015). Mitochondrial Ca^{2+} uptake by the voltage-dependent anion channel 2 regulates cardiac rhythmicity. *eLife*, *4*. https://doi.org/10.7554/eLife.04801

Shuvo, S. R., Ferens, F. G., & Court, D. A. (2016). The N-terminus of VDAC: Structure, mutational analysis, and a potential role in regulating barrel shape. *Biochimica et Biophysica Acta-Biomembranes*, *1858*, 1350–1361. https://doi.org/10.1016/j.bbamem.2016.03.017

Subedi, K. P., Kim, J.-C., Kang, M., Son, M.-J., Kim, Y.-S., & Woo, S.-H. (2011). Voltage-dependent anion channel 2 modulates resting Ca^{2+} sparks, but not action potential-induced Ca^{2+} signaling in cardiac myocytes. *Cell Calcium*, *49*, 136–143. https://doi.org/10.1016/j.ceca.2010.12.004

Szabadkai, G., Bianchi, K., Várnai, P., De Stefani, D., Wieckowski, M. R., Cavagna, D., … Rizzuto, R. (2006). Chaperone-mediated coupling of endoplasmic reticulum and mitochondrial Ca^{2+} channels. *The Journal of Cell Biology*, *175*, 901–911. https://doi.org/10.1083/jcb.200608073

Tan, W., & Colombini, M. (2007). VDAC closure increases calcium ion flux. *Biochimica et Biophysica Acta*, *1768*, 2510–2515. https://doi.org/10.1016/j.bbamem.2007.06.002

Trott, O., & Olson, A. J. (2010). AutoDock Vina: Improving the speed and accuracy of docking with a new scoring function, efficient optimization, and multithreading. *Journal of Computational Chemistry*, *31*, 455–461. https://doi.org/10.1002/jcc.21334

Ujwal, R., & Abramson, J. (2012). High-throughput crystallization of membrane proteins using the lipidic bicelle method. *Journal of Visualized Experiments*, *59*, e3383.

Ujwal, R., Cascio, D., Colletier, J.-P., Faham, S., Zhang, J., Toro, L., … Abramson, J. (2008). The crystal structure of mouse VDAC1 at 2.3 Å resolution reveals mechanistic insights into metabolite gating. *Proceedings of the National Academy of Sciences of the United States of America*, *105*, 17742–17747. https://doi.org/10.1073/pnas.0809634105

Waterhouse, A., Bertoni, M., Bienert, S., Studer, G., Tauriello, G., Gumienny, R., … Schwede, T. (2018). SWISS-MODEL: Homology modelling of protein structures and complexes. *Nucleic Acids Research*, *46*, W296–W303. https://doi.org/10.1093/nar/gky427

Zachariae, U., Schneider, R., Briones, R., Gattin, Z., Demers, J.-P., Giller, K., … Lange, A. (2012). β-barrel mobility underlies closure of the voltage-dependent anion channel. *Structure*, *20*, 1540–1549. https://doi.org/10.1016/j.str.2012.06.015

SUPPORTING INFORMATION

Additional supporting information may be found online in the Supporting Information section at the end of this article.

How to cite this article: Wilting F, Kopp R, Gurnev PA, et al. The antiarrhythmic compound efsevin directly modulates voltage-dependent anion channel 2 by binding to its inner wall and enhancing mitochondrial Ca^{2+} uptake. *Br J Pharmacol*. 2020;177:2947–2958. https://doi.org/10.1111/bph.15022

10 Acknowledgements

This thesis was conducted in the Cardiac Pharmacology Lab of the Walther Straub Institute of Pharmacology and Toxicology, LMU Munich, under supervision of Prof. Dr. Annette Nicke and Johann Schredelseker PhD.

I am deeply grateful to the director of the department, Prof. Dr. Thomas Gudermann for the opportunity to perform my doctoral thesis at the Walther-Straub-Institute, for providing excellent research facilities and stimulating scientific discussions.

I would like to express my sincere gratitude to my direct supervisor Johann Schredelseker PhD for the project design and continuous support, advice, encouragement and stimulating scientific input throughout my thesis.

I deeply thank Dr. Robin Kopp for his immense effort in the design and performing of the ligand-protein docking and for the helpful discussions about related questions.

I am deeply thankful to Paulina Sander and Anna Schedel for the time and effort they spent helping me every day and for their exceeding personal support and friendship – in good times and in bad.

I would like to thank Brigitte Meyerhofer for her continuous encouragement during the thesis and for her always helping hand.

I am thankful to all current and former members of this department for the friendly and supporting atmosphere that delighted the everyday work.

I thank the “Munich Heart Alliance” for providing personal and scientific financial support. Furthermore, I would like to acknowledge the Deutsche Forschungsgesellschaft DFG (DFG SCHR 1471/1-1 to J.S) and US National Institute of Health grant (R01GM071779 to O.K) for financial support.

I thank Wiebke Nadolni for her continuous encouragement during the thesis and for the friendship that survived since the first day at university.

Finally, my biggest thanks go to my family. Without your support I would not be where I am now. I thank you for always believing in me and supporting me in every situation. Thank you for supporting and encouraging me all these years during and prior to my thesis.